Toward a typology of river functioning: a comprehensive study of the particulate organic matter composition at the multi-river scale

Florian Ferchiche[1], Camilla Liénart[1], Karine Charlier[1], Jonathan Deborde[2,3], Mélanie Giraud[4], Philippe Kerhervé[5], Pierre Polsenaere[1,3], Nicolas Savoye[1*]

[1] Univ. Bordeaux, CNRS, EPHE, Bordeaux INP, UMR 5805 EPOC, F-33600 Pessac, France

[2] Univ. Pau & Pays Adour, CNRS, E2S UPPA – MIRA, UMR 5254 IPREM, F-64000 Pau, F-64600 Anglet, France

[3] Ifremer, COAST, F-17390 La Tremblade, France

[4] MNHN, CRESCO, Station Marine de Dinard, F-35800 Dinard, France

[5] Univ. Perpignan, CNRS, UMR 5110 CEFREM, F-66860 Perpignan, France

*Correspondence to: Nicolas Savoye (nicolas.savoye@u-bordeaux.fr) (+33)556223916
Université de Bordeaux - UMR 5805 EPOC - Station marine d'Arcachon - 2 rue du Professeur Jolyet - 33120 Arcachon

Keywords: river-estuary interface; particulate organic matter; stable isotopes; multi-ecosystem study.

Abstract

In riverine systems, particulate organic matter (POM) originates from various sources, each having its proper dynamics related to production, decomposition, transport and burial, resulting in a significant spatiotemporal heterogeneity in the POM pool. The current study, based on C and N elemental and isotopic ratios, applies Bayesian mixing models associated with statistical multivariate analyses to 1) quantify and examine relationships between POM composition and environmental forcings, and 2) draw a typology of river functioning based on POM composition and its seasonal dynamics.

Twenty-three temperate rivers accounting for a large diversity of environmental conditions were sampled fortnightly to monthly for one to seven years at their River-Estuary Interface (REI). Phytoplankton and labile terrestrial material occurred in all rivers, whereas sewage and refractory terrestrial material were present in only a few. At the twenty-three rivers scale, phytoplankton dominance was associated with agricultural surfaces, while labile terrestrial material was linked to organic-rich leached soil and refractory terrestrial matter to steep catchments with little soil. Seasonal dynamics were primarily driven by phytoplankton growth, river discharge (labile terrestrial material), and sediment resuspension (refractory terrestrial material).

A statistical regionalisation defined four types of river dynamics: (1) systems whose POM is dominated by labile terrestrial material year-round; (2) systems whose POM is composed of labile and refractory terrestrial material, in addition to phytoplankton, showing variable seasonality; systems whose POM is composed of phytoplankton and labile terrestrial material (3) without and (4) with pronounced seasonality. This work offers a comprehensive understanding of POM composition, spatio-temporal dynamics and controlling factors at the REI in temperate climates, complementing similar work dedicated to coastal systems. Future work dedicated to estuaries is called to get a comprehensive understanding of POM composition, dynamics and drivers along the Land-Ocean Aquatic Continuum.

1. Introduction

The River-Estuary Interface (REI) is a crucial biogeochemical interface for understanding the transition between continental and coastal systems, beginning at estuaries, because of its key location within the Land-Ocean Aquatic Continuum (LOAC) (Bate et al., 2002). Indeed, rivers then estuaries are important filters for matters received from land, transporting and transforming organic matter and nutrients along their courses (Bouwman et al., 2013; Dürr et al., 2011; Middelburg and Herman, 2007). These processes are fundamental in understanding global biogeochemical cycles (Regnier et al., 2013), as these matters directly fuel coastal ocean trophic networks (Dagg et al., 2004). However, in a Human-impacted world, anthropogenic activities and disturbances can modify natural matter fluxes. For example, damming rivers directly impacts nutrient flows (Wang et al., 2022) and sediment transportation (Kang et al., 2021). Indirectly, land use in river basins can lead to changes in the river matter quality (Lambert et al., 2017).

In aquatic systems, particulate organic matter (POM), i.e., non-mineral particles, is composed of different sources that originate from different compartments: phytoplankton, macrophytes from the aquatic systems, as well as plant litter, soil and petrogenic particles from terrestrial compartments and even treated and untreated anthropogenic organic matter (Ke et al., 2019; Sun et al., 2021; Zhang et al., 2021). Depending on its composition, POM exhibits different levels of lability, i.e., different levels of biogeochemical reactivity and bioavailability. For instance, phytoplankton is usually considered highly labile, and thus highly biogeochemically reactive and bioavailable for primary consumers, while terrestrial POM is usually considered more and more refractory through degradation processes, thus lightly biogeochemically reactive and poorly bioavailable for the food webs (Brett et al., 2017; David et al., 2005; Etcheber et al., 2007). In other words, the determination and quantification of POM composition (i.e., the relative proportion of each source composing the POM) allow a better understanding of biogeochemical cycles and trophic ecology in aquatic systems (e.g., Grunicke et al., 2023; Minaudo et al., 2016). Nevertheless, POM composition and concentration are not only involved in biogeochemical and biological processes (e.g., primary production, remineralisation, feeding) but also undergo other processes inside and at the interface of the aquatic compartment (Canuel and Hardison, 2016). River hydrology is a key factor controlling POM composition and concentration. The ~~geological~~ bedrock and soil characteristics of each catchment, together with climatic conditions, shape the erosional processes, leading to great variabilities in hydrodynamics, terrestrial material quality and quantity and phytoplankton growth conditions (Dalzell et al., 2007; Hilton et al., 2010; Lebreton et al., 2016). This variability leads to shifts in POM source origins (Arellano et al., 2019; Barros et al., 2010). Additionally, anthropogenic disturbances can directly or indirectly affect seasonal as well as long-term patterns of POM composition and concentration. For instance, a decrease in nutrient load affects phytoplankton production and biomass (Minaudo et al., 2015), agricultural surface

alters soil properties and erosion and consequently soil particle export to rivers, damming alters river hydromorphology and consequently particle dynamics and export (Kang et al., 2021; Zhang et al., 2021), etc.

This dependency of POM composition and concentration to physical, biogeochemical and biological processes and their responses to environmental conditions and characteristics (Bonin et al., 2019; Falkowski et al., 1998; Field et al., 1998; Galeron et al., 2017; Goñi et al., 2009; Lebreton et al., 2016) may lead to distinguishing different types of rivers, i.e., the likeliness of rivers to carry preferential sources. For instance, highly turbid systems are more likely to carry refractory materials (Savoye et al., 2012), while eutrophicated rivers carry high biomass of phytoplankton (Hounshell et al., 2022; Minaudo et al., 2015), and contrasting processes can lead to a mixture between different detrital sources, as soil matter vs. fresh terrestrial plants (Ogrinc et al., 2008). However, to date, no study clearly determined typologies of river dynamics based on POM composition and its seasonal variability.

To distinguish POM sources and quantify their contribution to POM composition, different tools such as elemental and isotopic ratios, pigments or specific compounds like fatty acids or alkanes can be used (e.g., Chevalier et al., 2015; Liénart et al., 2020, 2017; Savoye et al., 2012). Elemental and isotopic ratios are usually considered robust and allow the quantification of POM composition in this kind of study (e.g., Liénart et al., 2016; Onstad et al., 2000; Wang et al., 2021). Indeed, they usually allow the discrimination of, e.g., riverine phytoplankton, terrestrial POM and wastewater POM (Ke et al., 2019), and they can be used for running mixing models that quantify the proportion of the different sources in a POM mixture (Parnell et al., 2013). However, studies using mixing models for quantifying POM composition in river systems are still quite scarce (e.g., Ferchiche et al., 2025, 2024; Kelso and Baker, 2022, 2020; Zhang et al., 2021).

Within the scope of better understanding the role of the LOAC in modifying matter fluxes and quality, the present study gathered published data and results from 23 rivers at the river-estuary interface with the aim of 1) quantifying the POM composition of each river, 2) describing the seasonal variations of this composition, 3) determining the drivers of the seasonal variability within each river and the spatial variability among the 23 rivers, and then 4) determining a typology of river dynamics according to their POM composition and dynamics. This study is the first that precisely quantify POM composition in numerous and various temperate river systems in a world region (here, Western Europe) and classify river types according to POM composition and dynamics.

2. Materials and methods

Twenty-three temperate rivers were studied at their river-estuary interface (i.e., right upstream of the tidal influence). All the data come from published studies or national open databases. To minimize the heterogeneity of the datasets in terms of sampling strategy, we have considered

for this study the datasets only when 1) C/N ratio along with isotopic ratio of carbon and/or nitrogen were available, 2) particulate matter characteristics like, suspended particulate matter (SPM), particulate organic carbon (POC), particulate nitrogen (PN) or chlorophyll *a* (chl *a*) were also available, 3) datasets exhibited at least a monthly temporal resolution for one full year. When needed, published datasets were completed and harmonised thanks to national databases.

2.1.Study sites

The studied rivers and associated watersheds are all located in France (except the upper basin of the Rhône River) and distributed in all regions of the mainland. Three, fifteen and five of these rivers flow into the English Channel, the Atlantic Ocean and the Mediterranean Sea (Fig. 1). Even if located in a somewhat restricted area (Western Europe) at the global scale, they encompass large gradients of environmental characteristics (Tab. 1) for a temperate climate. For instance, the Loire River is one of the largest in Europe (length: 1006 km; watershed: 117,356 km²), while the littlest studied river is a very small stream of the Arcachon lagoon (length: 3 km; watershed: 18 km²). They encompass large gradients of river flow (annual mean: 0.3 m^3/s – 1572 m^3/s), turbidity (SPM annual mean: 2.7 mg/l – 40.9 mg/l) and trophic status (from oligotrophic to eutrophic rivers; chlorophyll *a* annual mean: 0.4 µg/l – 57.1 µg/l). At last, they undergo a gradient of anthropic pressures as illustrated by the proportion of artificial surfaces (0.1 % – 5.6 %) and agricultural areas (0 % – 86 %) in the watersheds (Fig. 1).

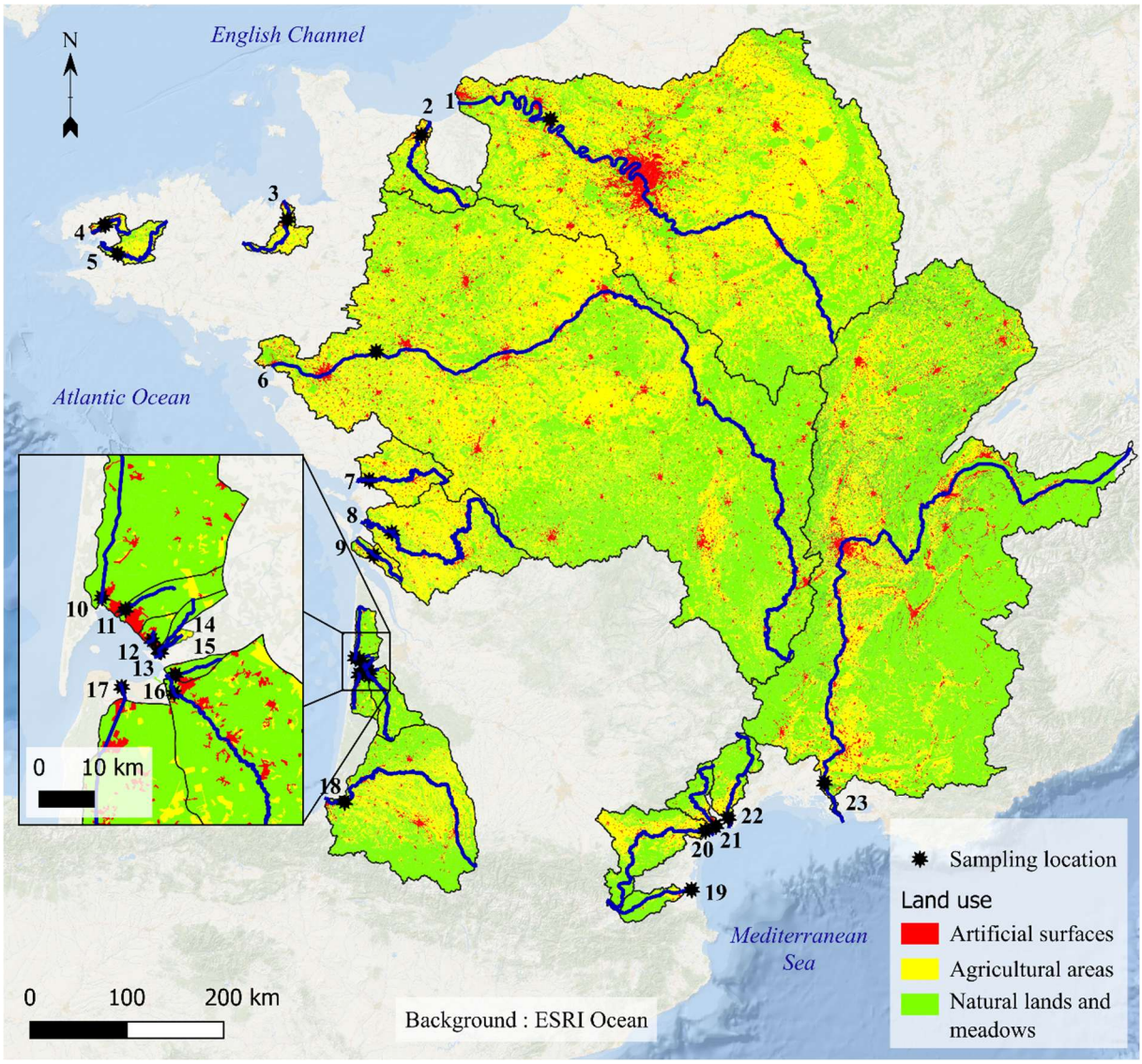

Figure 1 Studied rivers (thick blue lines), sampling locations (black stars) and watersheds (thin black lines), including the main land uses (red, yellow and green colours). 1: Seine; 2: Orne; 3: Rance; 4: Elorn; 5: Aulne; 6: Loire; 7: Sèvre niortaise; 8: Charente; 9: Seudre; 10: Canal du Porge; 11: Cirès; 12: Milieu; 13: Lanton; 14: Renet; 15: Tagon; 16: Leyre; 17: Canal des Landes; 18: Adour; 19: Têt; 20: Aude; 21: Orb; 22: Hérault; 23: Rhône. Background: ESRI Ocean

Table 1 Overview of river samplings and characteristics. Values are given as annual mean over the study period for river flow, temperature, suspended particulate matter (SPM) and chlorophyll *a* (chl *a*). Id: identification number; Number: number of sampling dates. River types were defined within the scope of the present study (see section 3.4).

River	Id	River type	Sampled period	Sampling Periodicity	Number	Latitude	Longitude	River length (km)	Catchment area (km²)	River flow (m3/s)	Water temperature (°c)	SPM (mg/l)	Chl *a* (µg/l)	References
Seine	1	IV	06/2014 to 06/2015	monthly	13	49.3067	1.2425	774	79000	496	15.0	21	2.8	Liénart et al., 2017, 2018
Orne	2	III	06/2014 to 06/2015	monthly	13	49.1797	-0.3491	169	2932	16	14.5	11	1.8	Liénart et al., 2017, 2018
Rance	3	IV	06/2014 to 05/2015	monthly	12	48.4916	-2.0014	103	1195	1.37	15.1	21	57.1	Liénart et al., 2017, 2018
Elorn	4	IV	01/2014 to 06/2015	monthly	17	48.4505	-4.2483	56	385	6	12.3	16	3.0	Liénart et al., 2017, 2018
Aulne	5	IV	01/2014 to 06/2015	monthly	17	48.2127	-4.0944	144	1875	30	14.4	7	3.3	Liénart et al., 2017, 2018
Loire	6	IV	10/2009 to 07/2012	bi-monthly	67	47.3920	-0.8604	1006	117356	630	14.1	19	18.7	Ferchiche et al., 2024
Sèvre	7	IV	03/2014 to 03/2015	monthly	13	46.3153	-1.0039	158	3650	3.72	15.7	13	3.8	Liénart et al., 2017, 2018
Charente	8	III	03/2014 to 03/2015	monthly	13	45.8680	-0.7131	381	9855	68	15.1	13	1.3	Liénart et al., 2017, 2018
Seudre	9	I	03/2014 to 09/2015	monthly	15	45.6740	-0.9331	68	855	1.81	14.3	17	0.5	Liénart et al., 2017, 2018
Porge	10	III	01/2008 to 02/2009	monthly	14	44.7898	-1.1612	57	222	3.48	13.3	12	5.0	Polsenaere et al., 2013
Cirès	11	I	02/2008 to 02/2009	monthly	13	44.7598	-1.1107	12	45	0.58	12.2	5	0.4	Polsenaere et al., 2013
Renet	12	I	02/2008 to 02/2009	bi-monthly	23	44.7144	-1.0441	3	18	0.56	12.9	10	0.6	Polsenaere et al., 2013
Lanton	13	I	02/2008 to 02/2009	monthly	13	44.7002	-1.0244	15	36	0.26	12.5	11	1.2	Polsenaere et al., 2013
Milieu	14	I	02/2008 to 02/2009	monthly	13	44.6973	-1.0225	7	21	0.58	12.7	7	0.4	Polsenaere et al., 2013
Tagon	15	I	02/2008 to 02/2009	bi-monthly	26	44.6590	-0.9891	10	30	0.64	12.6	13	1.3	Polsenaere et al., 2013
Leyre	16	I	01/2008 to 03/2010 and 02/2014 to 02/2015	bi-monthly or monthly	59	44.6263	-0.9961	116	1700	17	13.0	11	0.9	Dubois et al., 2012 / Polsenaere et al., 2013 / Liénart et al., 2017, 2018
Landes	17	III	02/2008 to 02/2009	monthly	12	44.6169	-1.1091	14	117	0.49	14.1	3	1.1	Polsenaere et al., 2013
Adour	18	III	04/2013 to 06/2014 and 05/2017 to	monthly	24	43.4988	-1.2949	308	16912	516	14.0	48	2.4	Liénart et al., 2016 / Deborde, 2019
Têt	19	II	01/2006 to 05/2010	monthly	52	42.7137	2.9935	115	1369	23	15.7	8	NA	Higueras et al., 2014
Hérault	20	II	01/2006 to 05/2010	monthly	52	43.3594	3.4354	148	2582	53	16.0	7	NA	Higueras et al., 2014
Orb	21	II	01/2006 to 05/2010	monthly	52	43.2850	3.2813	136	1585	23	15.7	8	NA	Higueras et al., 2014
Aude	22	II	01/2006 to 05/2010	monthly	52	43.2442	3.1527	223	5327	40	14.2	31	NA	Higueras et al., 2014
Rhône	23	II	12/2003 to 01/2011	monthly	105	43.6787	4.6212	812	95590	1572	15.9	41	1.9	Harmelin-Vivien et al., 2010 / Cathalot et al., 2013 / Higueras et al., 2014

2.2.Data origin

Regarding the core parameters (C/N ratio, $\delta^{13}C$, $\delta^{15}N$, water temperature, SPM, POC, PN, chl *a*), most of the data sets come from published studies (Canton et al., 2012; Cathalot et al., 2013; Dubois et al., 2012; Ferchiche et al., 2024; Harmelin-Vivien et al., 2010; Higueras et al., 2014; Liénart et al., 2016, 2017, 2018; Polsenaere et al., 2013), while most of additional parameters come from national databases (Tab. A1). When not available in the cited studies, concentrations of SPM, NO_3^-, NH_4^+ and PO_4^{3-}, pH and water temperature were retrieved from the *Naïades* database (https://naiades.eaufrance.fr/, consulted the 07/10/2023). Note that these parameters were not necessarily measured or sampled exactly at the same location or date for *Naïades* as in the cited studies. In that case, the location was chosen as close as possible to the study location and data values were time-interpolated to match the study date. Meteorological variables (air temperature, zonal and meridional wind, irradiance; used to qualify photosynthetic favourable conditions or wind-induced resuspension) come from Météo France, the French meteorological service. Wind data were received originally as direction and speed. To remove the angular bias, they were combined using scalar products to get zonal and meridional wind speeds, which range between minus and plus infinity (see Lheureux et al., 2022, for more details). River flows (used to qualify the hydrodynamics forcing) were retrieved from the *Banque Hydro* database (https://www.hydro.eaufrance.fr/, consulted the 07/10/2023) or from Polsenaere et al. (2013) for the small streams.

Catchment properties were retrieved when available for the 23 rivers. Land use proportions originate from the Corine Land Cover database (https://www.statistiques.developpement-durable.gouv.fr/corine-land-cover-0, consulted the 10/01/2024). Soil organic carbon data originate from the SoilTrEC database (https://esdac.jrc.ec.europa.eu/content/predicted-distribution-soc-content-europe-based-lucas-biosoil-and-czo-context-eu-funded-1, consulted the 10/01/2024). Net erosion soil data originate from the WaTEM/SEDEM database (https://esdac.jrc.ec.europa.eu/content/estimate-net-erosion-and-sediment-transport-using-watemsedem-european-union, consulted the 10/01/2024). Strahler numbers originate from the CARTHAGE database (https://www.sandre.eaufrance.fr/atlas/srv/api/records/c1d89cc3-c530-4b0d-b0ae-06f5ebf7997d, consulted the 15/08/2025). Useful water reserve values come from the GSF database (Le Bas, 2025). ~~Geological~~ Bedrock, ~~and~~ soil types, granulometry and slope come from the GISSOL database (gathered by great ~~geological~~ bedrock and soil types according to the provided legend; INRA, 2025). Wastewater treatment capacities originate from the Eau France WFS services (https://services.sandre.eaufrance.fr/geo/odp?REQUEST=getCapabilities&service=WFS&VERSION=2.0.0, couche sa:SysTraitementEauxUsees, consulted the 15/08/2025). All these catchment data were pre-processed on a Geographical Information System to extract information for each catchment surface, then averaged or weighted (depending on continuous or semi-quantitative data) to characterise each system with a value.

It should be noted that a complete study was already dedicated to the Loire River and reported as a companion article (Ferchiche et al., 2024). Consequently, the results are not reported in the present study but are used for multi-system comparisons (Fig. 5 and 7, and corresponding text).

2.3.Determination of sources signatures

To run mixing models for quantifying POM composition, it is previously needed to 1) determine sources of POM, and 2) associate elemental and isotopic signatures to these sources. In riverine systems, autochthonous (mainly phytoplankton) and allochthonous (resuspended sediment, terrestrial fresh litter or rock-derived soil) are the main sources that are usually considered as fuelling the POM (e.g., Ferchiche et al., 2024; Pradhan et al., 2016; Sarma et al., 2014). Nevertheless, sewage POM may also contribute (Higueras et al., 2014). Consequently, phytoplankton, labile and refractory terrestrial POM and sewage POM were considered as potential sources in this study.

Phytoplankton cannot be easily picked up from bulk particles to measure its elemental and isotopic ratios. Therefore, the method developed and used by Savoye et al. (2012), Liénart et al. (2017) and Ferchiche et al. (2024) was applied here. It consists of determining the elemental and isotopic ratios from a subset of the bulk dataset. Briefly, phytoplankton-dominated POM is characterised by a low POC/chl *a* ratio (≤ 200 or even ≤ 100 g/g; Savoye et al., 2003 and references therein). Thus, elemental and isotopic ratios of samples exhibiting a low POC/chl *a* ratio can be considered as good estimates of phytoplankton elemental and isotopic ratios. When the POC/chl *a* ratio is not available, samples exhibiting a high PN/SPM ratio can be used. Additional constraints may be used to minimise potential overlap between phytoplankton and terrestrial elemental and isotopic signatures. Phytoplankton elemental and especially isotopic ratios may vary deeply over time and space depending on primary production intensity and potential limiting factors, nutrient origin, etc. (e.g., Miller et al., 2013; Savoye et al., 2003). When existing, this variability has to be taken into account to avoid using elemental and isotopic signatures that are not valid at the time or location of the sampling. This could be performed by using regressions between elemental and/or isotopic ratios and environmental variables (see Ferchiche et al., 2024; Liénart et al., 2017; Savoye et al., 2012). At last, when no samples exhibit a low POC/chl *a* ratio, samples exhibiting the lowest (even if high) POC/chl *a* ratios can be used, but the data should first be corrected for the contribution of the terrestrial POM using Equations 1-3.

$$\delta^{13}C_{sample} = ([POC]_{phytoplankton} \times \delta^{13}C_{phytoplankton} + [POC]_{terrestrial} \times \delta^{13}C_{terrestrial}) / [POC]_{sample} \quad \text{(eq. 1)}$$

$$[POC]_{phytoplankton} = [\text{chl } a]_{sample} \times (\text{POC/chl } a)_{mean} \quad \text{(eq. 2)}$$

$$[POC]_{terrestrial} = [POC]_{sample} - [POC]_{phytoplankton} \quad \text{(eq. 3)}$$

where $(POC/chl\ a)_{mean}$ is the mean POC/chl *a* ratio of the samples used to determine phytoplankton signatures. Similar equations are used for the N/C ratio, $\delta^{15}N$ and C/N ratio, but using PN instead of POC for $\delta^{15}N$ and C/N ratio.

Elemental and isotopic signatures of terrestrial POM can be estimated by directly measuring elemental and isotopic ratios in a sample like soil, rocks or vascular plants (e.g., Sarma et al., 2014). However, this does not take into account the reworking of this material within the river system, which can affect these signatures (Hou et al., 2021). Thus, similarly to phytoplankton, elemental and isotopic signatures of terrestrial POM can be estimated using subsets of bulk data, following the approach of Savoye et al. (2012), Liénart et al. (2017) and Ferchiche et al. (2025, 2024). Labile terrestrial POM is usually characterised by high POC/chl *a* and C/N ratios and low POC/SPM ratios (Etcheber et al., 2007; Savoye et al., 2003 and references therein). However, during its decay in aquatic systems, terrestrial POM is colonised by bacteria (low C/N ratio), resulting in a consortium terrestrial POM + bacteria of lower C/N ratio than the original terrestrial POM (Etcheber et al., 2007; Savoye et al., 2012). Finally, one can discriminate two kinds of terrestrial POM: refractory terrestrial POM, characterised by high POC/chl *a* and C/N ratios and very low POC/SPM ratio, and quite labile terrestrial POM characterised by high POC/chl *a* ratio, intermediate C/N ratios and low POC/SPM ratio (Etcheber et al., 2007; Savoye et al., 2012). Thus, subsets of high POC/chl *a* ratio can be selected to determine the elemental and isotopic signatures of terrestrial POM. The C/N ratio can be used to discriminate labile from refractory terrestrial POM. When no samples exhibit a high POC/chl *a* ratio, samples exhibiting the highest (even if quite low) POC/chl *a* ratio can be used, but the data should first be corrected for the contribution of the phytoplankton POM using Equations 1-3.

Elemental and isotopic ratios of riverine POM can exhibit a departure from a simple phytoplankton-terrestrial POM mixing. In the present study, this was the case in only two rivers. For the Têt River, the elemental and isotopic signature of anthropogenic POM was available in Higueras et al. (2014). It consisted of analyses of POM sampled in the wastewater treatment plant (WWTP) closest to the sampling site. For the Orb River, the signatures were estimated using the sample exhibiting the lowest $\delta^{15}N$, typical of anthropogenic POM (Ke et al., 2019).

The estimation of POM-source signatures was performed independently for each river, except for some of the tributaries of the Arcachon Lagoon (rivers 11 to 15), where data sets were gathered, thanks to very similar characteristics (same δ13C of dissolved inorganic carbon; Polsenaere et al., 2013), to get a larger subset of data for estimating elemental and isotopic signatures more accurately. All criteria used for defining the above-described subsets are reported in Table 2.

Table 2 Elemental and isotopic signatures of POM sources and criteria used to choose the data subset to determine them. When the signature did not vary over time, average ± standard

deviation are reported. When the signature did vary over time, minimum and maximum values, standard deviations, as well as equations are reported. The types of mixing models performed for each river are also indicated (carbon mixing models were performed using $\delta^{13}C$ and N/C ratio, or only $\delta^{13}C$; nitrogen mixing models were performed using $\delta^{15}N$ and C/N ratio; mixed mixing models were performed using $\delta^{13}C$, $\delta^{15}N$ and N/C ratio). POC% (or PN%) = Particulate Organic Carbon (or Particulate Nitrogen) to Suspended Particulate Matter ratio (%); C/N = POC/PN ratio (mol/mol); chla = chlorophyll *a* (µg/l); phaeo = phaeopigments (µg/l); conduc = conductivity (µS); temp = water temperature (°C); Q7 = mean of past seven days river flow; NO_3^- = nitrate ($mg(NO_3^-)/l$).

River	Source discriminants				Model performed			Labile terrestrial matter				Refractory terrestrial matter			
	Labile terrestrial matter	Refractory terrestrial matter	Phytoplankton	WWTP's POM	Carbon	Nitrogen	Mixed	$\delta^{13}C$	$\delta^{15}N$	C/N	N/C	$\delta^{13}C$	$\delta^{15}N$	C/N	N/C
Seine	C/N > 10		POC/chla < 200		X	X		-28.5 ± 0.3	6.6 ± 0.9	10.6 ± 0.3	0.093 ± 0.002				
Orne	C/N > 11		POC/chla < 500		X	X		-28.4 ± 0.3	5.8 ± 1.0	12.4 ± 0.4	0.082 ± 0.003				
Rance	POC/chla > 200 and chla < 10		POC/chla < 150		X	X		-26.8 ± 0.2	6.1 ± 0.7	8.8 ± 0.4	0.113 ± 0.007				
Elorn	C/N > 12		POC/chla < 200		X	X		-28.4 ± 0.7	5.8 ± 0.9	13.0 ± 0.8	0.077 ± 0.005				
Aulne	C/N > 11		POC/chla < 200 and C/N < 9		X	X		-28.9 ± 0.8	5.8 ± 0.8	12.1 ± 1.1	0.08 ± 0.008				
Loire	POC/chla > 500		POC/chla < 200		X	X		-28.1 ± 0.1	5.9 ± 0.3	10.3 ± 0.2	0.097 ± 0.002				
Sèvre Niortaise	C/N > 14		POC/chla < 300		X			-28.0 ± 0.4			0.057 ± 0.040				
Charente	C/N > 12		POC/chla < 300		X	X		-29.0 ± 0.4	4.7 ± 0.2	14.5 ± 0.5	0.069 ± 0.002				
Seudre	POC/chla > 2000 and C/N > 12		POC/chla < 1000		X			-28.5 ± 0.1							
Porge	C/N > 15		$\delta^{13}C$: POC/chla < 100 ; N/C : mean of Cirès to Landes		X			-26.5 ± 1.1			0.050 ± 0.007				
Cirès / Renet / Milieu / Lanton / Tagon	C/N > 15 and chla < 1		POC/chla < 1000 and POC% > 10		X			-28.5 ± 0.5			0.053 ± 0.013				
Leyre	C/N > 15 and chla < 1		POC/Chla < 1000. $\delta^{13}C$ < 28.59 and POC% > 10		X			-28.3 ± 0.5			0.06 ± 0.005				
Landes	C/N > 12		POC/Chla < 600. $\delta^{13}C$ < -29.1		X			-29.1 ± 0.4			0.075 ± 0.002				
Adour	POC/chla > 3000		POC/chla < 200		X			-26.0 ± 0.9			0.099 ± 0.008				
Têt	C/N > 11.5	POC% < 4.25	PN% > 2. $\delta^{13}C$ < 26 and δ15N > 5	Measured			X	-26.0 ± 0.2	3.7 ± 0.6	12.2 ± 0.5	0.082 ± 0.002	-26.0 ± 0.6	6.7 ± 1.4	5.8 ± 1.4	0.180 ± 0.045
Aude	C/N > 12	Q7 > 70	PN% > 1 or 2 and C/N < 6				X	-28.1 ± 0.6	6.3 ± 0.1	15.3 ± 1.6	0.066 ± 0.007	-28.0 ± 0.7	4.7 ± 0.4	7.3 ± 1.0	0.139 ± 0.018
Orb	C/N > 10		PN% > 2. $\delta^{15}N$ > 4.06	Lower $\delta^{15}N$			X	-27.1 ± 0.4	3.7 ± 0.4	10.5 ± 0.3	0.095 ± 0.350				
Hérault	C/N > 12	Q > 45	PN% > 2				X	-27.7 ± 0.2	6.1 ± 0.7	13.7 ± 1.2	0.073 ± 0.007	-27.8 ± 0.4	4.7 ± 0.6	8.2 ± 1.5	0.124 ± 0.019
Rhône	C/N > 12	POC% < 1.25	C/N < 6.68 and $\delta^{15}N$ > 3.92				X	-26.4 ± 1.3	5.2 ± 1.0	17.0 ± 3.2	0.061 ± 0.012	-25.9 ± 0.4	3.1 ± 0.8	8.8 ± 3.1	0.119 ± 0.032

Table 2 (continued)

River	Phytoplankton							WWTP's POM			
	$\delta^{13}C$ + equations		$\delta^{15}N$ + equations		C/N	N/C + equations		$\delta^{13}C$	$\delta^{15}N$	C/N	N/C
Seine	-32.8 ± 1.1		8.4 ± 1.7		7.4 ± 0.7	0.136 ± 0.012					
Orne	-31.4 ± 0.8		4.3 ± 0.8		6.6 ± 1.3	0.141 ± 0.010					
Rance	[-31.4;-25;6] ± 1.7	$5.7x10^{-4}$×[chla+phaeo]²-0.04×[chla+phaeo]-30.6	[4.7;11.4] ± 0.7	-0.28×[NO_3^-]+12.7	6.2 ± 0.4	0.161 ± 0.010					
Elorn	-27.4 ± 0.3		6.9 ± 0.5		10.0 ± 0.9	0.101 ± 0.007					
Aulne	-28.1 ± 0.2		8.6 ± 0.2		8.2 ± 0.2	0.122 ± 0.003					
Loire	[-30.6;-25.0] ± 0.9	$5x10^{-4}$×[chla+phaeo]²-0.02[chla+phaeo]-0.39[chla/phaeo]-27.9	[3.0;10.4] ± 1.2	$4.2x10^{-4}$[chla]²-0.08[chla]+8.2	7.2 ± 0.6	0.140 ± 0.011					
Sèvre Niortaise	[-35.7;-29.2] ± 1.0	-258×exp([chla+phaeo]²/16055)-0.15×[temp]+229				[0.106;0.145] ± 0.006	2.9x10 ^{3}×[chla+phaeo] + 0.1				
Charente	-30.8 ± 0.03		7.5 ± 1.6		6.6 ± 0.3	0.152 ± 0.006					
Seudre	-33.3 ± 0.1										
Porge	-33.6 ± 0.4					0.128 ± 0.008					
Cirès / Renet / Milieu / Lanton / Tagon	-34.9 ± 0.4					0.133 ± 0.006					
Leyre	-30.1 ± 0.3					0.140 ± 0.016					
Landes	-29.9 ± 0.3					0.112 ± 0.010					
Adour	-28.2 ± 0.6					0.111 ± 0.010					
Têt	[-29.7;-27.8] ± 0.6	-5.2×10^{-3}[temp]² +0.08×[temp]-27.5	[5.3;13.3] ± 1.8	5.53×[temp]-5.5	5.6 ± 0.7	0.181 ± 0.021		-26.3 ± 0.1	-0.7 ± 0.1	6.3 ± 0.3	0.160 ± 0.017
Aude	[-32.6;-27.8] ± 0.6	-0.21×[temp]-26.5	[5.2;10.6] ± 1.6	$-1.13\times\delta^{13}C$-26.2	5.0 ± 0.8	0.205 ± 0.033					
Orb	[-30.7;-23.4] ± 0.6	-0.19×[temp]-26.0	[4.9;8.4] ± 0.6	8.44-(3.63×(conduc-505))/(conduc-111)	4.8 ± 0.9	0.213 ± 0.039		-27.1 ± 0.4	1.9 ± 1.9	3.7 ± 3.7	0.270 ± 0.270
Hérault	[-31.5;-27.5] ± 1.0	-0.19×[temp]-26.0	[6.3;10;9] ± 1.3	$3.6x10^{-2}$×[temp]²-1.15×[temp]+14.6	5.0 ± 0.7	0.203 ± 0.031					
Rhône	-27.8 ± 1.2		5.6 ± 0.8		5.5 ± 0.8	0.180 ± 0.030					

2.4.Quantification of POM composition

POM composition was quantified using a Bayesian mixing model ('*simmr*' R package version 0.4.5, Govan and Parnell, 2023), which solves the equations system based on bulk and source POM elemental and isotopic signatures. Mixing models were computed for each sampling date of each river (Tab. 1), using carbon ($\delta^{13}C$ and N/C ratio, Eq. 4, 7, 8), nitrogen ($\delta^{15}N$ and C/N ratio, Eq. 5, 6, 8), and/or a combination of three ($\delta^{13}C$, $\delta^{15}N$ and N/C ratio, Eq. 4, 5, 7, 8) tracers. From the three mixing models performed for each sampling date and river (carbon, nitrogen or mixed), one model was selected as the best estimation of bulk POM data. It should be noted that N/C and C/N ratios give information on the mixing of C and N, respectively (Perdue and Koprivnjak, 2007). We used at least the same number of equations as unknowns (sources) to avoid running underdetermined models that result in large uncertainty in model outputs(Phillips et al., 2014). Equations of the models were:

$$\delta^{13}C_{mixture} = x_1\,\delta^{13}C_{source\,1} + x_2\,\delta^{13}C_{source\,2} + x_3\,\delta^{13}C_{source\,3} + x_4\,\delta^{13}C_{source\,4} \quad \text{(Eq. 4)}$$

$$\delta^{15}N_{mixture} = x_1\,\delta^{15}N_{source\,1} + x_2\,\delta^{15}N_{source\,2} + x_3\,\delta^{15}N_{source\,3} + x_4\,\delta^{15}N_{source\,4} \quad \text{(Eq. 5)}$$

$$C/N_{mixture} = x_1\,C/N_{source\,1} + x_2\,C/N_{source\,2} + x_3\,C/N_{source\,3} + x_4\,C/N_{source\,4} \quad \text{(Eq. 6)}$$

$$N/C_{mixture} = x_1\,N/C_{source\,1} + x_2\,N/C_{source\,2} + x_3\,N/C_{source\,3} + x_4\,N/C_{source\,4} \quad \text{(Eq. 7)}$$

$$x_1 + x_2 + x_3 + x_4 = 1 \quad \text{(Eq. 8)}$$

As there was no *a priori* knowledge of sources contributions to the POM mixture, the models were set with an uninformative prior (1, 1, 1, 1) following a Dirichlet distribution (all sources have an equal probability to contribute to the mix; Phillips et al., 2014). Model runs were set following the recommendations of Phillips et al. (2014). Models outputs were evaluated with Gelman-Rubin diagnostic (verification of chain convergence) and predictive distributions to ensure the good fit of the models to the observed data. Models outputs are given as medians. Absolute uncertainties for the models varied from 1 to 18 % (range of average for each river) with an overall average of 8 % (all models).

2.5.Forcings at local and multi-system scales

Environmental forcings driving POM composition were determined using redundancy analysis (RDA; 'dudi.pca' and 'pcaiv' functions; R package {ade4} version 1.7-19). RDA summarises multiple linear regressions between the response variable (POM composition: mixing model outputs) and a set of explanatory variables (environmental forcings) to assess causality links (Legendre et al., 2011). RDAs were performed at single-river and multi-river scales. Regarding the multi-river scale, the annual mean POM composition of each river was used to determine the drivers of spatial (i.e., between-rivers) variations of POM composition.

The proxies of the environmental forcings were chosen to directly or indirectly reflect the forcings that affect the processes occurring in the river and the adjacent ecosystems and influencing POM source inputs. To homogenise the data sets for running the single-river RDAs, the same combination of twelve parameters (see Table A2) was used for each river. They are linked to primary production (chlorophyll *a*, phaeopigments, temperature, pH, ammonium, nitrate, phosphate, irradiance), upstream and lateral, natural and/or anthropogenic inputs (river flow, rain, SPM, ammonium, nitrate, phosphate), and resuspension (SPM, zonal and meridional wind energy). For the multi-river RDA, environmental proxies were selected to reflect processes occurring at large spatial scales and in the river basin. Forty parameters (See Fig. A6) were used. They are linked to water quality (conductivity, nitrates), climate setting (river flow, latitude, longitude, air temperature, precipitation, zonal, meridional and total wind energy), ~~hydromorphology~~ geomorphology (river length and flow, basin surface area and~~,~~ slope, Strahler number), land use coverage (agricultural areas, artificial surfaces, forest and seminatural areas, wetlands and water bodies), catchment –soil properties (organic carbon content, net erosion,

granulometry, useful water reserves[1]), soil type (~~podzol~~acidic, brown, organic and hydromorphic soil), ~~geological~~ bedrock type (~~alluvial~~alluvial/unconsolidated deposits, calcareous and marl rocks, clayey materials, detrital formations, sandy materials, ~~loamy~~loess, crystalline and metamorphic rocks, volcanic rocks and other/organic materials), and urban pressure (WWTP capacities, WWTP capacities to river flow ratio)~~.~~. From this initial list of proxies, some were removed to limit the auto-correlation (use of the Variance Inflation Factor, Borcard et al., 2011) and to improve the adjusted R^2 of each RDA analysis (Tab. A2 and Fig. A6).

2.6. Typology of river dynamics

Rivers were classified based on POM composition and their temporal dynamics by performing a regionalisation analysis as in Liénart et al. (2018) (Fig. A1). This method, based on multivariate cluster analysis (Souissi et al., 2000), allows to consider the temporal (seasonal) variations specific to each river in addition to the spatial (between-rivers) component. The regionalisation analysis was based on POM composition data (i.e., proportions of sources) computed for each river and each month. When the sampling was fortnightly, averages were performed to get one value per month. When more than one year was sampled, a standard year was chosen. Nevertheless, to check if the choice of one year over the other ones would modify the typology, another regionalisation was performed using all available years for all rivers. This regionalisation also allowed to check if a river can shift from one type to another type depending on year and associated environmental conditions (inter-annual variability of type belonging). Also, in order to check if the over-representation of the small rivers and streams fuelling the Arcachon Bay would bias the typology, a third regionalisation was performed, reducing the numbers of these rivers from 8 to 3 (and especially from 6 to 1 regarding rivers of Type I). The results (Fig. 5, Fig. A7) are very similar, indicating the robustness of the method.

A contingency matrix (rivers, sources, months) was created from monthly values of source contributions (i.e., mixing model outputs). For each month, a dendrogram was performed, and ten cut-off levels were considered. Then, for each cut-off level, similarities between stations were identified within the twelve-monthly dendrograms. Ultimately, global similarities between rivers were computed using a fuzzy cluster that returns probabilities of membership of each river to each cluster type. The best number of river types, i.e., river dynamics typology, was determined considering the best Dunn coefficient (Dunn, 1974) and Silhouette score (Rousseeuw, 1987).

3. Results

[1] Useful water reserve corresponds to the water ~~that is~~ retained by the soil and that is~~-~~ useful for plants. It is calculated from soil thickness and granulometry (Le Bas, 2025)

Hereafter, four rivers (Rance, Charente, Milieu and Hérault Rivers) were selected and considered as representative of each type of studied river (see section 3.4). Thus, most of the results are illustrated using these four rivers. Graphs of all the other rivers are reported in the supplementary material.

3.1. Contrasting seasonalities in river characteristics

As stated in section 2.1, the 23 studied rivers encompassed large gradients of environmental characteristics, as illustrated by the lowest and highest annual means of river flow (0.3 and 1572 m^3/s; Lanton and Rhône Rivers), water temperature (12.3 to 17.1 °C; Cirès and Têt Rivers), SPM (2.7 and 40.9 mg/l; Cirès and Rhône River), POC (0.3 and 5.1 mg/l; Hérault and Loire Rivers) and chlorophyll *a* (0.4 to 57.1 µg/l; Cirès and Rance Rivers) concentrations as well as POC/chl *a* (199 and 6444 g/g; Loire and Leyre Rivers) and C/N (5.9 and 20.3 mol/mol; Têt and Lanton Rivers) ratios; this was less contrasting among rivers for $\delta^{13}C$ (-30.2 and -26.2 ‰; Sèvre and Têt Rivers) and especially $\delta^{15}N$ (4.0 and 8.0 ‰; Leyre and Rance Rivers) (Fig. 2, A2).

As generally observed in rivers from mid-latitude, the studied rivers exhibited clear seasonal patterns in water temperature with lower and higher values in winter and summer, respectively. However, such clear seasonal patterns were not always recorded for all the parameters, as there were contrasting patterns of seasonal variability among rivers. Indeed, the seasonal variability of river flow was quite smooth (e.g., the Rance and Charente Rivers) with a higher flow in winter/spring and lower flow in summer/fall for some rivers, whereas it was highly pulsed for some others with constant low levels marked by short and strong floods (e.g., $53 m^3/s$ in mean but $1169 m^3/s$ in flood time for the Hérault River) (Fig. 2). Overall, one can distinguish rivers that are characterized by high concentrations of chlorophyll *a* and clear seasonal patterns of most parameters (e.g., 53 µg/l of chlorophyll *a* in mean ranging from 3 to 135 µg/l in the Rance River) from rivers characterized by low concentrations of chlorophyll *a*, high POC/chl *a* and low seasonal variability for most of the parameters (e.g., 1.1 µg/l of chlorophyll *a* in mean ranging from 0.7 to 1.7 µg/l in the Milieu River) and from rivers that are characterized by high seasonal variability of most parameters but without a clear seasonal pattern (e.g., Hérault River). Other rivers exhibited intermediate behaviour (e.g., Charente River) (Fig. 2, A2). Usually, Rance-like rivers exhibited high concentrations of chlorophyll *a* in spring/summer associated with POC/chl *a* ratio lower than 200 g/g, C/N ratio lower than 8 mol/mol and low $\delta^{13}C$ (down to -31 ‰ or -33 ‰; e.g., Seine River, Fig. A2). In contrast, Milieu-like rivers exhibited high POC/chl *a* (> ~ 700 g/g) and C/N ratio (> 15 mol/mol) and quite constant $\delta^{13}C$ (~-29 – -28 ‰) all year round (e.g., Cirès and Renet Rivers). These rivers are tributaries of the Arcachon Lagoon. Hérault-like rivers flowing into the Mediterranean Sea exhibited highly and suddenly variable C/N ratios (4 – 17 mol/mol), $\delta^{13}C$ (~-33 – -26 ‰) and $\delta^{15}N$ (~2 – 12 ‰) (e.g., Aude and Orb Rivers; Fig. A2).

387

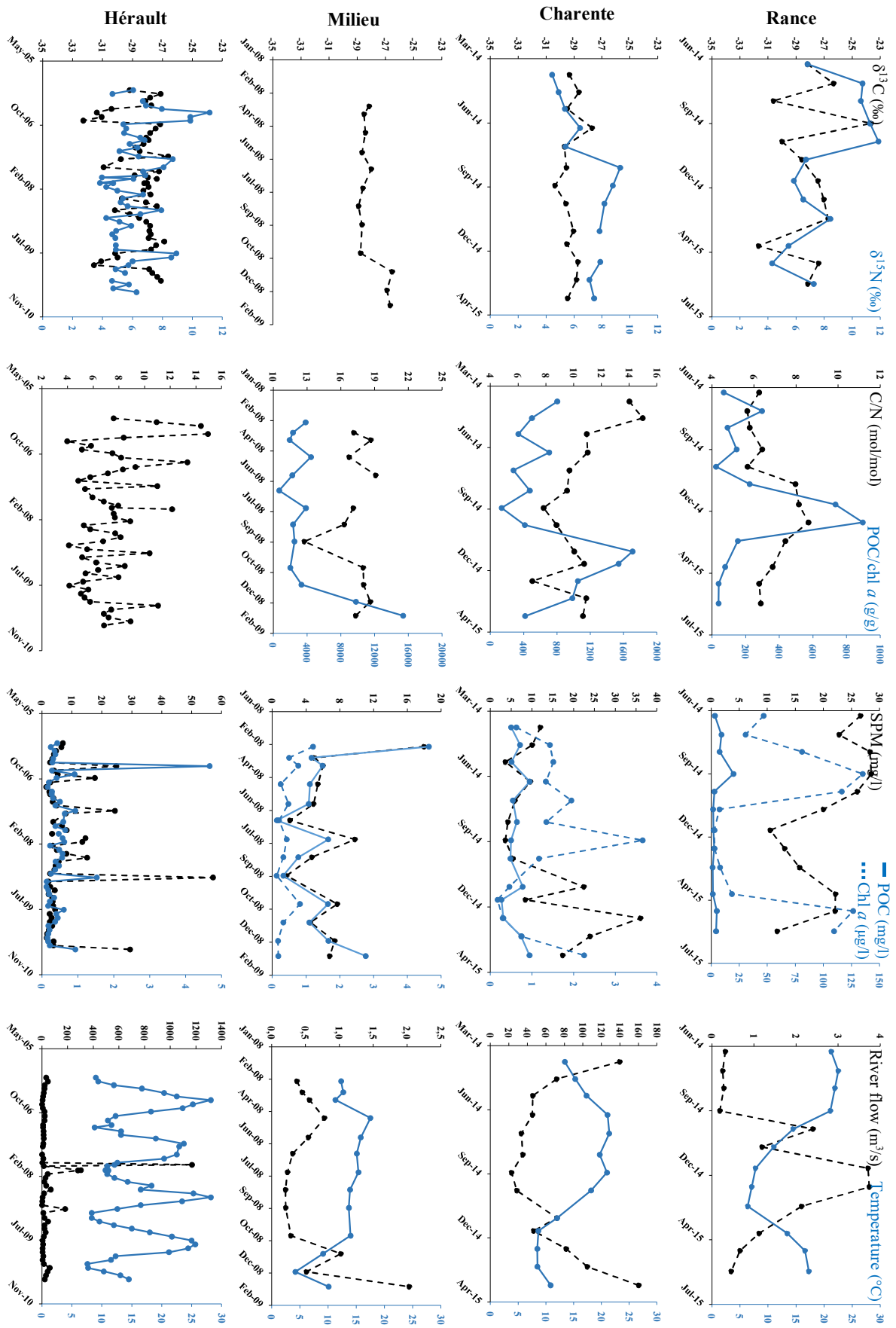
Rance
Charente
Milieu
Hérault
δ13C (‰)
δ15N (‰)
C/N (mol/mol)
POC/chl a (g/g)
SPM (mg/l)
POC (mg/l)
Chl a (µg/l)
River flow (m3/s)
Temperature (°C)

Figure 2 Temporal variations of matter characteristics for representative rivers along the studied periods for $\delta^{13}C$ (left axis; black dotted line) and $\delta^{15}N$ (right axis; blue line) (first column); C/N (left axis; black dotted line) and POC/chl a (right axis; blue line) ratios (second column); SPM(left axis; black dotted line), POC (right axis; blue line) and chl *a* (right axis; blue dotted line) concentrations (third column) and river flow (left axis; black dotted line) and temperature (right axis; blue line) (fourth column).

3.2. Elemental and isotopic signatures of POM sources

Elemental and isotopic signatures of phytoplankton were estimated for each of the twenty-three rivers (Tab. 2, Fig. 3 and A3). Most of them (all of them for the C/N ratio) were found to be constant over time. Their annual mean values varied between -34.9 ‰ (some tributaries of the Arcachon Lagoon) and -27.4 ‰ (Elorn River) for $\delta^{13}C$, between 4.3 ‰ (Elorn River) and 8.6 ‰ (Aulne River) for $\delta^{15}N$ and between 4.8 mol/mol (Orb River) and 10.0 mol/mol (Elorn River) for the C/N ratio. Some of them varied over time along with pigment concentration and ratio or with temperature for $\delta^{13}C$, and with pigment concentration (chlorophyll *a* and/or phaeopigments), nitrate concentration, temperature, $\delta^{13}C$ or conductivity for $\delta^{15}N$ (Tab. 2). The range of temporal variability was usually 4-6 ‰ for $\delta^{13}C$ and $\delta^{15}N$. Overall, phytoplankton signatures are comprised between -35.6 and -23.8 ‰ for the $\delta^{13}C$ and between 3.0 and 13.2 ‰ for the $\delta^{15}N$.

All other signatures were found to be constant over time (Tab. 2 and A2, Fig. 3 and A3) but may differ between rivers. Signatures mean annual values of labile terrestrial POM were comprised between -29.1 and -26.0 ‰ for the $\delta^{13}C$, between 3.7 and 6.6 ‰ for the $\delta^{15}N$ and between 8.8 and 17.0 mol/mol for the C/N ratio. Signatures mean annual values of refractory terrestrial POM were comprised between -28.0 and -25.9 ‰ for the $\delta^{13}C$, between 3.1 and 6.7 ‰ for the $\delta^{15}N$ and between 5.8 and 8.8 mol/mol for the C/N ratio. Signatures mean annual values of sewage POM were -27.1 and -26.3 ‰ for $\delta^{13}C$, 1.9 and -0.7 ‰ for $\delta^{15}N$ and 3.7 and 6.3 mol/mol for C/N ratio for Orb and Têt Rivers, respectively.

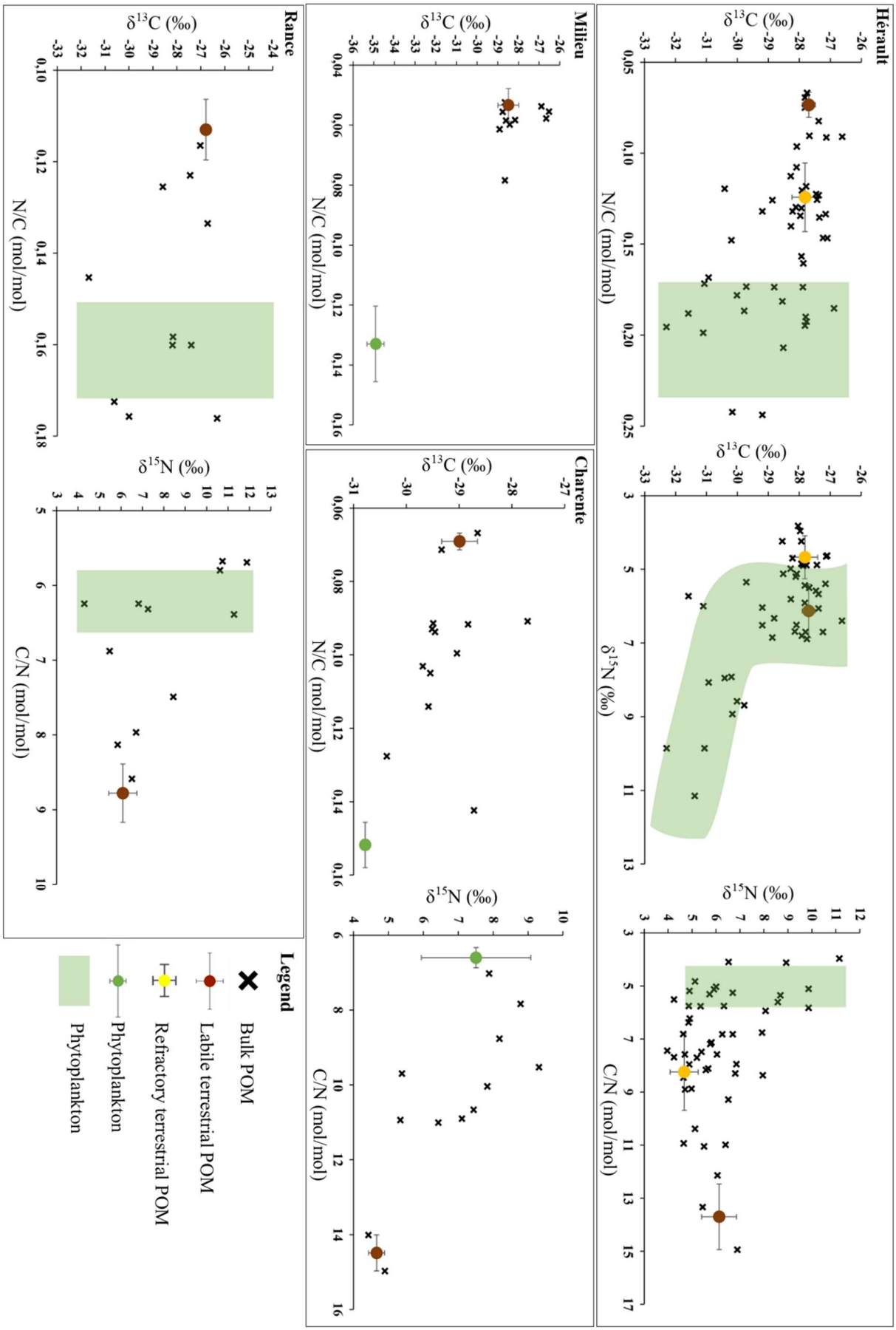
Hérault
Milieu
Charente
Rance
δ13C (‰)
N/C (mol/mol)
δ15N (‰)
C/N (mol/mol)
Legend
Bulk POM
Labile terrestrial POM
Refractory terrestrial POM
Phytoplankton
Phytoplankton

414

Figure 3 $\delta^{13}C$, $\delta^{15}N$, N/C or C/N values of bulk POM (black crosses) and sources. The latter are presented as closed circles (average) and bars (standard deviation) when the signatures were constant over time and by colored area when at least one of the proxies was variable over time (see Table 2). This colored area corresponds to the dispersion of the values, including their uncertainties.

3.3.Dynamics of particulate organic matter composition

Particulate organic matter composition resulting from mixing models outputs is presented hereafter, for each river, as the relative contribution of each source to the POM pool (Fig. 4). Among rivers whose POM is composed of only two sources (terrestrial POM and phytoplankton), one can distinguish rivers with terrestrial-dominated POM (e.g., Milieu River: terrestrial POM accounted for 94 ± 3 % of the mixture) to rivers of intermediate POM composition (e.g., Charente and Rance Rivers where phytoplankton accounted for 34 ± 10 % and 62 ± 10 % of the mixture, respectively). All these rivers flow into the English Channel and the Atlantic Ocean. The rivers whose POM is composed of three or four sources flow into the Mediterranean Sea. In these rivers, terrestrial POM is present as refractory and labile materials. The contribution of labile terrestrial POM ranged between 16 ± 15 % (Têt River) and 46 ± 21 % (Orb River), and of refractory terrestrial POM between 21 ± 9 % (Rhône River) and 39 ± 15 % (Aude River). The contribution of phytoplankton ranged between 34 ± 15 % (Aude River) and 51 ± 30 % (Hérault River) for the Mediterranean rivers. The fourth source of POM was the WWTP's POM. It was identified as a source in the Orb and Têt Rivers and accounted for 15 ± 6 % and 10 ± 7 % in these two rivers, respectively. Regarding temporal variations of POM composition, some rivers exhibited clear seasonal patterns, whereas others revealed a homogeneous composition over the annual cycle (Fig. 4). The rivers where POM was highly dominated by terrestrial POM (Seudre, Cirès, Renet, Lanton, Milieu, Tagon, Leyre Rivers) showed almost no seasonal variability. In contrast, some rivers like the Rance, the Elorn or the Aulne River showed a clear seasonal pattern with the dominance of terrestrial material in winter and phytoplankton in summer. At last, other rivers exhibited less clear (e.g., Landes, Porge, Charente Rivers) or even no clear seasonal pattern but a quite stochastic variability over the annual cycle (e.g., Sèvre, Adour, Aude, Orb).

It should be noted that the above is valid for carbon and mixed as well as nitrogen models (cf. Tab. 2; Fig. 4 and A4).

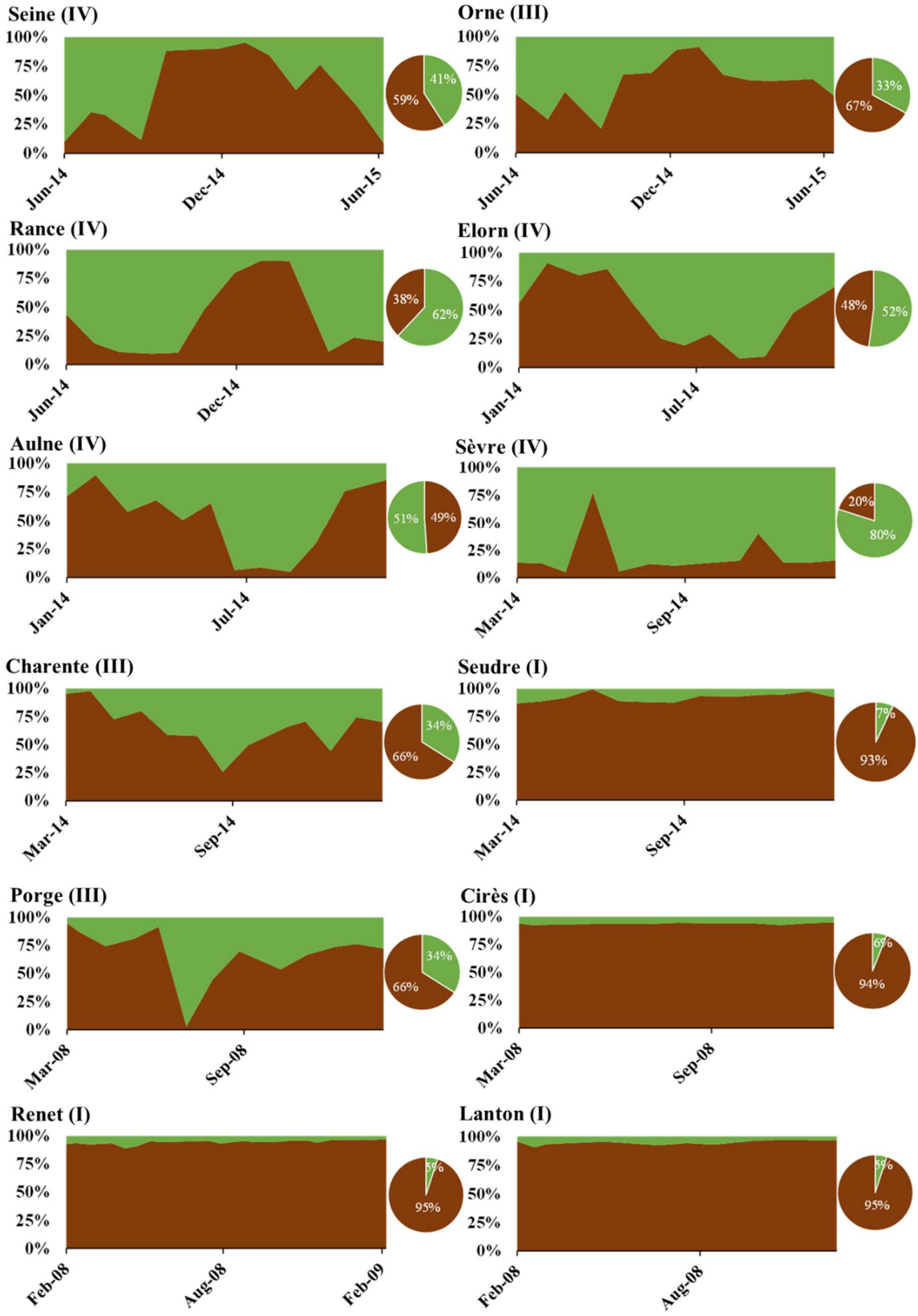
Seine (IV)
100%
75%
50%
25%
0%
Jun-14
Dec-14
Jun-15
41%
59%
Orne (III)
Jun-14
Dec-14
Jun-15
33%
67%
Rance (IV)
Jun-14
Dec-14
38%
62%
Elorn (IV)
Jan-14
Jul-14
48%
52%
Aulne (IV)
Jan-14
Jul-14
51%
49%
Sèvre (IV)
Mar-14
Sep-14
20%
80%
Charente (III)
Mar-14
Sep-14
34%
66%
Seudre (I)
Mar-14
Sep-14
7%
93%
Porge (III)
Mar-08
Sep-08
34%
66%
Cirès (I)
Mar-08
Sep-08
6%
94%
Renet (I)
Feb-08
Aug-08
Feb-09
5%
95%
Lanton (I)
Feb-08
Aug-08
5%
95%

446

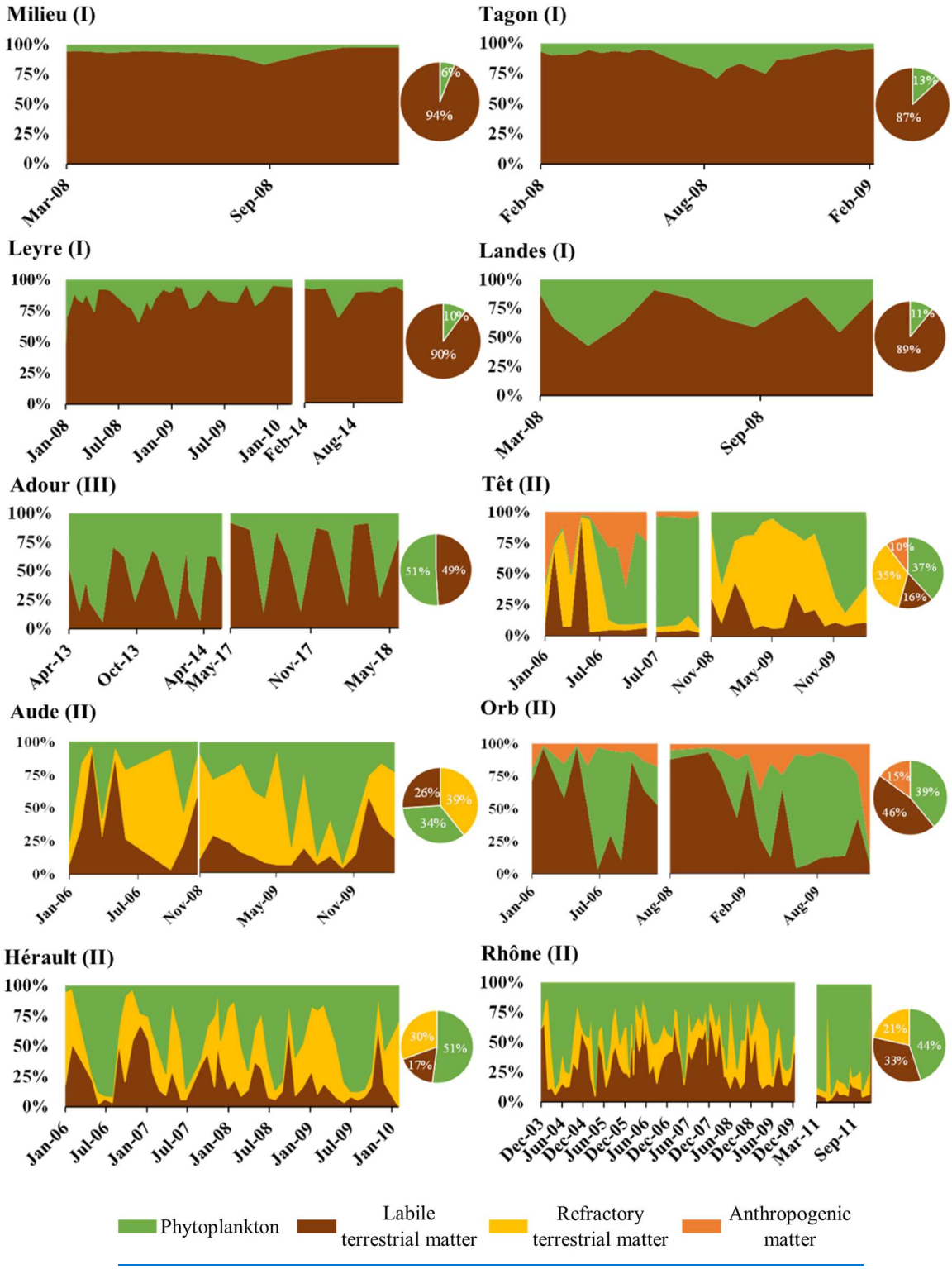

Figure 4 Temporal dynamic (rectangle graphs) and (inter-)annual mean (pie charts) of POC source proportions. Sources are phytoplankton (green), labile terrestrial material (brown), refractory terrestrial material (yellow) and anthropogenic POM (orange).

3.4. Typology of river dynamics

Four types of river dynamics were determined by the regionalisation analysis based on river POM compositions and their temporal dynamics (Fig. 5). The seven rivers (Renet, Cirès, Lanton, Milieu, Seudre, Tagon and Leyre River), mainly belonging to Type I, were characterised by terrestrial-dominated POM and no/low seasonality. Six of them are small streams/rivers flowing to the Arcachon Lagoon. The five rivers (Aude, Hérault, Têt, Rhône and Orb River), mainly belonging to Type II, were characterised by the co-occurrence of labile and refractory terrestrial POM and large temporal variability, but, except for the Hérault River, without a clear seasonal pattern. They all flow to the Mediterranean Sea. The five rivers (Porge, Adour, Charente, Orne and Landes River), mainly belonging to Type III, were composed of phytoplankton and terrestrial POM, and exhibited moderate seasonality. Type III is clearly an intermediary between Type I and Type IV. These five rivers flow to the Atlantic Ocean or the English Channel. Among the seven rivers flowing to the Arcachon Lagoon, the two that mainly belong to Type III are man-managed streams and flow through lakes, contrary to the six other ones, which mainly belong to Type I and are natural streams that do not flow through lakes. Finally, the six rivers (Rance, Elorn, Aulne, Loire, Seine and Sèvre River) mainly belonging to Type IV were composed of phytoplankton and terrestrial POM, and exhibited high seasonality. These six rivers flow to the Atlantic Ocean or the English Channel. It should be noted that the regionalisations performed using all sampled years for all rivers (Fig. A7) resulted in the same typology and in the same type for each river, whatever the sampling year. The only exception is the Leyre River, which switched from Type III in 2008 to Type I in 2009.

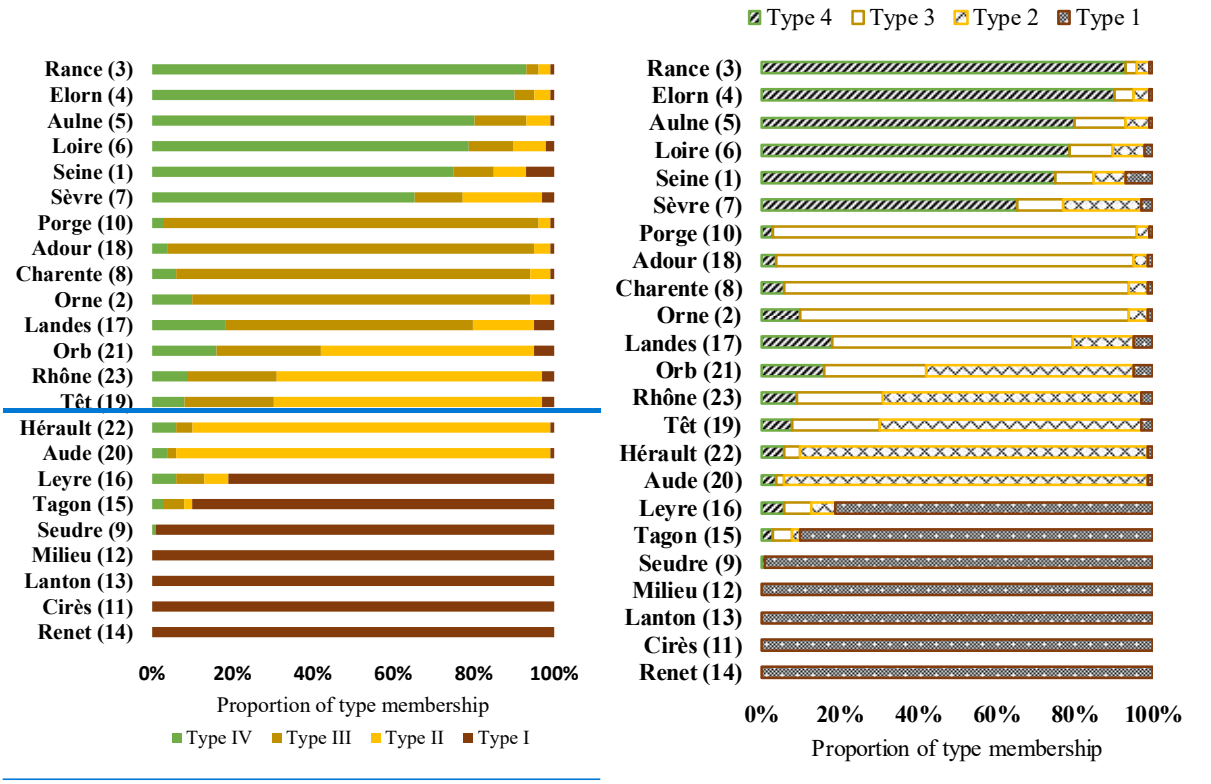

Figure 5 Typology of river dynamics following a hierarchical cluster analysis on POM source proportions. The percentages of membership for each type attributed to each river are shown.

3.5. Environmental forcings driving POM composition

One redundancy analysis was performed for each river to relate environmental parameters, considered as proxies of drivers, to the POM composition, i.e., to assess the drivers of the temporal variability of POM composition for each river (Fig. 6 and A5). It should be kept in mind that the POC or PN concentration of each source was used for these analyses and not the relative proportion of the sources. In type-I rivers, i.e., rivers characterised by terrestrial-dominated POM and no/low seasonality, terrestrial POM is usually linked to river flow and/or SPM concentration (e.g., Milieu River on Fig. 6, Leyre and Tagon Rivers in Fig. A5). However, this feature is not always clear since the POM of these rivers is always dominated by terrestrial material, regardless of the environmental conditions. In type-II rivers, i.e., rivers characterised by the co-occurrence of labile and refractory terrestrial POM and large temporal variability, phytoplankton POM is usually positively linked to temperature and negatively linked to river flow, whereas labile and refractory terrestrial POM are both positively linked to SPM and/or river flow. Precisely, labile terrestrial POM is usually better linked to river flow and refractory terrestrial POM to SPM (e.g., Hérault River in Fig. 6 and Rhône River in Fig. A5). In the Têt River, anthropogenic POM was linked to nitrate concentration (Fig. A5). In rivers characterised by phytoplankton and terrestrial-POM composition with moderate (Type III) or high (Type IV) seasonality, terrestrial POM was almost always positively linked to river flow and/or SPM concentration, while phytoplankton was usually linked with chlorophyll *a* concentration (e.g., Charente and Rance Rivers on Fig. 6, Landes and Seine Rivers on Fig. A5).

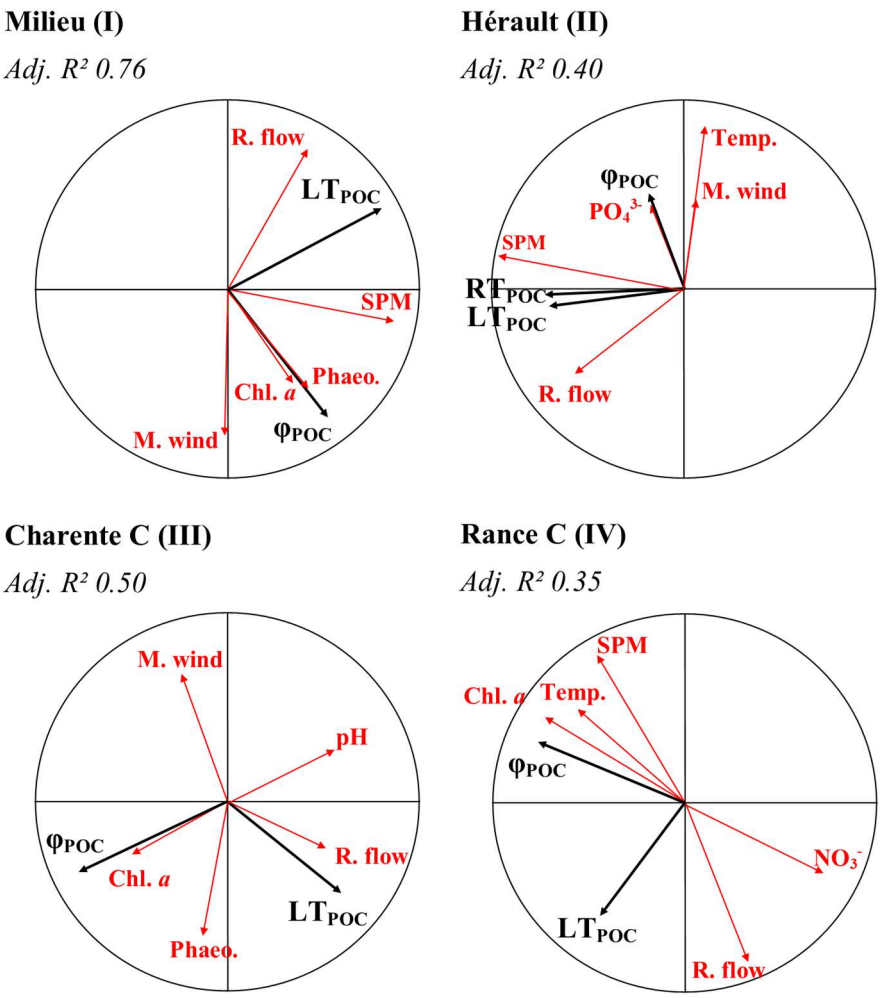

Figure 6 Redundancy analyses (correlation circles) of rivers standing for each type of river. Black arrows represent explained variables (concentration of POC sources) and red arrows represent explaining variables (environmental variables). River types are recalled (Roman numerals). LT_{POC} = Labile terrestrial POC; RT_{POC} = Refractory terrestrial POC; φ_{POC} = Phytoplankton POC; Chl *a* = chlorophyll a; Phaeo. = phaeopigments; M. wind = meridional wind; Z. wind = zonal wind; R. flow = river flow; Temp. = temperature; Irrad. = Irradiance; NH_4^+ = ammonium; NO_3^- = nitrate; PO_4^{3-} = phosphates; Adj. R^2 = adjusted R^2.

At last, another RDA was performed, gathering all rivers to relate environmental parameters to the mean annual POM composition at the multi-river scale (Fig. 7). As anthropogenic POM was only detected in two rivers (Orb, Têt), it was not included in the multi-river analysis to avoid analysis bias. At this scale, phytoplankton is strongly positively correlated to agricultural surfaces and conductivity, labile terrestrial material to soil organic carbon content and ~~podzol~~ acidic soil coverage, and refractory terrestrial material to catchment slope; refractory terrestrial material is also negatively correlated to soil useful water reserves ~~of water~~ (all correlations are

significant; Fig. A6). Note that the phytoplankton and labile terrestrial matter, as well as their related environmental variables, are negatively correlated.

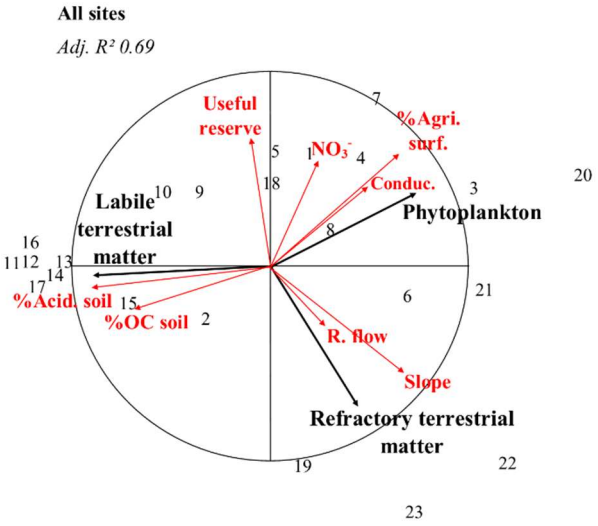

Figure 7 Multi-river redundancy analysis. Black arrows represent explained variables (relative proportions), red arrows represent explaining variables (environmental variables), and numbers are river identifiers (cf. Fig.1). R. flow = river flow; %OC soil = percentages of organic carbon in soil; NO_3^- = nitrates concentration; Useful reserve = Useful water reserve in soil; Conduc. = conductivity; %Agri. Surf. = Proportion of agricultural surface; %Acid. soil = Proportion of ~~podzol~~ acidic soil coverage; Slope = Catchment slope; Adj. R^2 = adjusted R^2.

4. Discussion

4.1. Bulk POM and source signatures in temperate rivers

Over the 23 studied rivers, $\delta^{13}C$, $\delta^{15}N$, and C/N ratios of bulk POM ranged between -35.2 and -24.5 ‰, -0.3 and 12.6 ‰, and 3 and 23.4 mol/mol, respectively. This corresponds to usual values recorded for riverine POM over temperate systems, except for the lowest C/N ratios (Ferchiche et al., 2024; Kendall et al., 2001; Ogrinc et al., 2008).

In the present study, isotopic and elemental signatures of terrestrial POM and phytoplankton were determined from subsets of the bulk data sets following the approaches of Savoye et al. (2012), Liénart et al. (2017) and Ferchiche et al. (2025, 2024). It has the double advantage of 1) taking into account the reworking of terrestrial POM within the river and thus discriminating labile from refractory terrestrial POM, and 2) taking into account the variability of phytoplankton signature over time, due to differences in growth conditions (see below). Labile terrestrial POM mainly appears during high river flow (Fig. 6 and A5; Savoye et al., 2012) and is usually composed of riparian litter (e.g., Veyssy et al., 1998). In the studied rivers, $\delta^{13}C$, $\delta^{15}N$ and C/N ratio of labile terrestrial POM ranged between -28.9 ± 0.8 ‰ and -26 ± 0.9 ‰, 3.7 ± 0.6 ‰ and 6.6 ± 0.9 ‰, and 8.8 ± 0.4 and 17 ± 3.2 mol/mol, respectively. These values are very similar to values found in other temperate systems like the Gironde Estuary ($\delta^{13}C$ = -28.7 ± 0.9

‰; Savoye et al., 2012), the Sava River ($\delta^{13}C$ = -28 ± 5 ‰; $\delta^{15}N$ = 5 ± 2 ‰; C/N = 33 ± 15 mol/mol; Ogrinc et al., 2008) or Taiwanese rivers ($\delta^{13}C$ = -26.6 ± 1.8 ‰; C/N = 31.1 ± 23.4 mol/mol; Hilton et al., 2010) and very similar to direct measurement of C3 plants ($\delta^{13}C$ = -28.1 ± 2.5 ‰; O'Leary, 1981 and references therein; $\delta^{13}C$ = -28 ± 1.3 ‰; $\delta^{15}N$ = 0.8 ± 2.9 ‰; C/N = 39.6 ± 25.7 mol/mol; Dubois et al., 2012; $\delta^{13}C$ = -27.9 ± 0.1 ‰; Fernandez et al., 2003). Refractory terrestrial POM is terrestrial POM that has undergone large reworking within river water, river sediment or even the estuarine maximum turbidity zone (e.g., Etcheber et al., 2007; Veyssy et al., 1998). In the studied rivers where it was found, $\delta^{13}C$, $\delta^{15}N$ and C/N ratios of refractory terrestrial POM ranged between -28 ± 0.7 ‰ and -25.9 ± 0.4 ‰, 3.2 ± 0.8 ‰ and 6.7 ± 1.4 ‰, and 5.8 ± 1.4 and 8.8 ± 3.1 mol/mol, respectively. These values are very similar to the large gradient of refractory POM origins found in other temperate systems like the Gironde Estuary (France) (resuspended sediment, $\delta^{13}C$ = -25.2 ± 0.3 ‰; $\delta^{15}N$ = 5.5 ± 0.4 ‰; C/N = 8.5 ± 0.8 mol/mol; Savoye et al., 2012), Taiwanese rivers (petrogenic POM, $\delta^{13}C$ = -23.6 ± 1.1 ‰; C/N = 6.5 ± 1.6 mol/mol; Hilton et al., 2010) and in the Pearl River (China) (soil, $\delta^{13}C$: between -28.3 ± 0.8 ‰ and -21.7 ± 0.7 ‰; C/N: between 8.9 ± 1.1 and 17.9 ± 3.6 mol/mol; Yu et al., 2010).

Isotopic signatures of phytoplankton vary depending on biogeochemical conditions and processes like nutrient availability and utilisation, growth rate and limitation (e.g., Fry, 1996; Liénart et al., 2017; Lowe et al., 2014; Miller et al., 2013; Savoye et al., 2003; Sigman et al., 2009; Yan et al., 2022) and can be estimated using measured environmental parameters (Ferchiche et al., 2024, 2025; Liénart et al., 2017; Savoye et al., 2012). For the seven rivers where phytoplankton isotopic signatures were found variable over time, phytoplankton $\delta^{13}C$ or $\delta^{15}N$ were correlated to: concentrations and ratio of chlorophyll *a* and phaeopigments, water temperature, nitrate concentration and/or conductivity (Tab. 2). Chlorophyll *a* and phaeopigments concentrations are direct proxies of phytoplankton fresh and degraded biomasses and are related to phytoplankton growth and decay, two processes that increase phytoplankton $\delta^{13}C$ (Golubkov et al., 2020; Michener and Kaufman, 2007 and references therein). Similar processes may explain phytoplankton-$\delta^{15}N$ increase with chlorophyll *a* increase. An increase in water temperature accelerates bio-mediated carbon remineralisation processes, bringing a lower $\delta^{13}C$ value than CO_2 coming from water-atmosphere equilibration and rock-leaching CO_2 (Polsenaere et al., 2013 and references therein). Consequently, phytoplankton $\delta^{13}C$ decreases as phytoplankton uses remineralised CO_2 and thus as water temperature increases. Phytoplankton $\delta^{15}N$ depends on N-nutrient origin and availability (Savoye et al., 2003 and references therein). Especially, it increases with nutrient concentration decrease (Sigman et al., 2009) as reported for the Rance River (Tab. 2). Water conductivity could be considered as a proxy of water mass and thus of nitrate origin. This may explain the relationship between phytoplankton $\delta^{15}N$ and water conductivity in the Orb River (Tab. 2).

In the studied rivers, phytoplankton $\delta^{13}C$, $\delta^{15}N$ and C/N ratio ranged between -34.9 ± 0.4 and -23.8 ± 0.6 ‰, 4.3 ± 0.8 and 13.2 ± 1.8 ‰, and 4.8 ± 0.9 and 10 ± 0.9 mol/mol, respectively. This is similar to values reported for the Loire River, another French river ($-30.6 \leq \delta^{13}C \leq -25.0$ ‰; $3.0 \leq \delta^{15}N \leq 10.4$ ‰; C/N = 7.2 ± 0.6 mol/mol: Ferchiche et al., 2024), but narrower ranges can be found in the literature. In the Sava River (Eastern Europe), phytoplankton signature was -30.4 ± 2.1 ‰, 5.0 ± 1.5 ‰ and 6.5 ± 1.5 mol/mol for $\delta^{13}C$, $\delta^{15}N$ and C/N ratio, respectively (Ogrinc et al., 2008), similar to that of Indian ($\delta^{13}C$ = -30.6 ± 1.7 ‰, $\delta^{15}N$ = 7.0 ± 2.3 ‰; Gawade et al., 2018) and Texan ($\delta^{13}C$ = -31,4 ‰; Lebreton et al., 2016) rivers. Lower $\delta^{13}C$ values (≤ -32 ‰) were also found (Finlay et al., 2010; Hellings et al., 1999; Sato et al., 2006; Savoye et al., 2012). However, values of elemental and isotopic ratios for riverine phytoplankton are scarce in the literature. Indeed, it is not easy to estimate the phytoplankton signature since it cannot be separated from other particles. Thus, literature estimates may not be perfectly representative of the variability of phytoplankton isotopic signatures.

4.2. Watershed characteristics drive spatial dynamics of POM composition

At the annual scale, we observed deep variations between studied rivers regarding the mean POC proportion of the different sources (5 ≤ phytoplankton ≤ 80 %; 17 ≤ labile terrestrial POC ≤ 95 %; 0 ≤ refractory terrestrial POC ≤ 39 %).

Interestingly, phytoplankton proportions were highly correlated to the proportion of agriculture surface areas and conductivity and in a less extent to river nitrate concentration (Fig. 7). Such relationship between agriculture surface and phytoplankton is well-known, as agricultural activities increase nutrient inputs to river bodies (Khan and Mohammad, 2014), leading to better conditions for phytoplankton growth (Dodds and Smith, 2016; Minaudo et al., 2015).

Also interestingly, the proportions of labile terrestrial matter were positively correlated to soil organic carbon content, soil erosion, the ~~podzol~~ acidic soil coverage and sandy ~~rock~~ material coverage (Fig. 7, Fig. A6), indicating a strong relationship between terrestrial matter in rivers and soil nature with undecomposed and fresh detrital matter (McCorkle et al., 2016). They are also negatively correlated to phytoplankton proportions and their related environmental parameters. Rivers which POM is dominated by labile terrestrial POM (mainly rivers of type I) flow through catchments dominated by sandy ~~rocks~~ material ~~and~~in ~~podzol~~podzol (an acidic soil type). This kind of soil is subject~~mitted~~ to soil erosion and releases large amounts of coloured dissolved organic carbon, favouring the input of terrestrial material (soil erosion) and disfavouring phytoplankton growth in the river water because of the turbidity due to the dissolved organic carbon (Canton et al., 2012; Polsenaere et al., 2013).

The proportions of refractory terrestrial matter are correlated to the catchment slope and negatively correlated to useful water reserve ~~of water~~ (Fig. 7, Fig. A6). Rivers for which POM

is partly composed of refractory terrestrial POM (most of the rivers of type II) flow through catchments of mountainous surfaces, which are associated with shallower, poorer topsoil and more outcropping bedrock (so a reduced ~~soil~~useful water reserve of the soil). It favours more reactive and abrupt transfer of water to the river, leading to enhanced episodes of sediment resuspension, as well as permitting a rock-derived POM weathering (Copard et al., 2018; Higueras et al., 2014; Yaalon, 1997).

4.3. Temporal dynamics of POM composition and river-dynamics typology

If average quantitative difference between rivers can be input to differences in the catchment characteristics (see section 4.2), seaso~~n~~nally, phytoplankton likely appears during spring and summer in favourable conditions, related to low discharge, high-temperature conditions and enough nutrients to support its growth, while in winter, high turbidity and low-temperature conditions limit its presence (Turner et al., 2022). . Terrestrial material likely appears during winter conditions, related to floods that transport great amounts of terrestrial material (Dalzell et al., 2007). Such a seasonal dichotomy between phytoplankton and terrestrial POM was clearly visible for most of the studied rivers (Fig. 4), especially for type-IV and type-III rivers, but even for some of those highly dominated by the labile terrestrial POM (e.g., Milieu and Tagon Rivers; Type-I rivers). This was illustrated by the relationships between phytoplankton POM and chlorophyll *a* concentration and/or temperature (as proxies of favourable conditions for phytoplankton production) on the one hand, and between labile terrestrial POM and river flow and/or SPM concentration on the other hand (Fig. 6 and A5). This dichotomy in POM composition was also reported in other similar studies (e.g., Kelso and Baker, 2020; Lu et al., 2016). In rivers where refractory terrestrial POM was present in addition to the labile one (type-II rivers), both terrestrial sources were linked to river flows and SPM concentrations. More precisely, it was interesting to see that the refractory terrestrial POM was more related to SPM concentration than river flow and inversely for the labile terrestrial POM. This indicates that labile and refractory terrestrial POM were preferentially associated with direct river input and sediment resuspension, respectively. The origin of the refractory terrestrial POM may be fossil/bedrock/petrogenic OM (e.g., Copard et al., 2022; Hilton et al., 2010; Sun et al., 2021) brought by river flow (in quantity undetectable in the bulk POM using our tools), especially in Type-II rivers which watersheds are characterized by high slopes (Fig. 7). This POM can be accumulated in downstream sediments and be resuspended (in quantity calculable in the bulk POM using our tools). Refractory terrestrial POM may also come from labile terrestrial POM brought by the river flow and then accumulated and reworked/decayed until refractory POM in the sediment (e.g., Etcheber et al., 2007; Savoye et al., 2012), which can be resuspended.

Sewage POM was detected in two of the studied rivers, but with different associated temporal dynamics. In the Têt River, because the former WWTP was dysfunctional, a new one replaced

it in late 2007 (https://www.assainissement.developpement-durable.gouv.fr/pages/data/fiche-060966136002, last visit 10/09/24). This explains the shift in sewage POM between the two studied periods (2006-2007 versus 2008-2010 without anthropogenic POM). In the Orb River, sewage POM was detected throughout the studied periods. The WWTP is located only a few kilometres upstream of the sampling site and is large enough (220,000 inhabitant equivalent) compared to the river flow (annual mean: $23 m^3/s$) to make the sewage POM detectable in the bulk POM using $\delta^{15}N$. Such a result is quite common for urban rivers (e.g., Kelso and Baker, 2020).

5. Synthesis, originality of the study and perspectives

The present study provides a comprehensive assessment of POM composition and its spatial and seasonal variability in temperate rivers. By including twenty-three rivers spanning a wide range of environmental conditions under a temperate climate, a river-dynamics typology is proposed based on POM composition and its temporal patterns. In type-I rivers, POM is dominated by labile terrestrial material throughout the year. This material is mainly associated with suspended particulate matter. Phytoplankton makes a slight contribution, especially during summer. Type-II rivers are characterised by the presence of both labile and refractory terrestrial material, along with phytoplankton. The variability between these sources over time is high, but seasonality is not always evident, although phytoplankton and terrestrial POM can dominate the POM composition during summer and winter, respectively. Nonetheless, if both terrestrial sources are primarily linked to river flow and SPM, a better coupling of refractory terrestrial POM with SPM indicates that this material is probably stored in sediments and resuspended, whatever its origin (soil, litter, petrogenic POM). In type-III rivers, POM consists of phytoplankton and labile terrestrial material. The seasonality of POM composition is not very pronounced, though the contribution of labile terrestrial POM is closely related to river flow. Type III is an intermediate between type I and type IV. In type-IV rivers, POM is also composed of phytoplankton and labile terrestrial material, but the seasonality is highly marked, with a clear shift from high phytoplankton contribution in summer to high terrestrial contribution in winter. Labile terrestrial POM remains closely associated with river flow. Beyond this typology, the main differences in POM composition between the studied rivers ~~is~~ are related to catchment inherent properties. The contribution of phytoplankton is correlated with the proportion of agricultural coverage, while the contribution of labile terrestrial POM is linked to leached OM-rich thick soil features and the refractory terrestrial POM to thin OM-poor soils with high rock-derived features.

The originality of the present study lies firstly in its approach. Even if C and N stable isotopes have been used for decades to investigate POM origins within river waters, the quantification of POM composition (i.e., the relative proportion of each source composing the POM) using mixing models, especially Bayesian mixing models, is not so common. Most previous studies

either use literature data for phytoplankton isotopic signature (e.g., Zhang et al., 2021) or use lake or autochthonous POM as a proxy of phytoplankton (e.g., Kelso and Baker, 2020). Also, most of these studies use direct measurements of soil or plants to assess the isotopic signature of terrestrial POM, although this material may rework within the water column or sediment, changing its elemental and isotopic values (e.g., Savoye et al., 2012). These approaches do not consider the temporal variability of phytoplankton and terrestrial material isotopic signatures. In the present study, we used the approach developed by Savoye et al. (2012) in an estuary, Liénart et al. (2017) in coastal systems, and Ferchiche et al. (2024, 2025) in a river to assess elemental and isotopic signatures from subsets of bulk POM and, when needed, empirical equations. This approach has the advantage of 1) using signatures dedicated to the sampling area and 2) taking into account the potential variability of these signatures over time, i.e., depending on environmental conditions for phytoplankton growth and its decay for phytoplankton and terrestrial POM. Especially, we discriminated labile from refractory terrestrial POM in some rivers, as Savoye et al. (2012) did in an estuary. Another great originality of the present study lies in the multi-system approach: studying 23 rivers in a single study allowed the detection of four types of river functioning regarding the POM composition and its temporal dynamics, which has not been performed before. It also highlights the great influence of land use (agriculture) and characteristics (erosion, organic carbon content, type of soil) on the POM composition of rivers. At last, the multi-parameter use of $\delta^{13}C$, $\delta^{15}N$, and C/N ratio allowed either to perform mixing models with up to four end-members or to study POC and PN composition separately. It showed that POC and PN display very similar compositions and dynamics in rivers. Overall, this study, which focuses on the River-Estuary Interface, brings meaningful information for the comprehension of C and N cycles along the LOAC and especially the behaviour, dynamics and drivers of POM that leaves the river and enters the estuary.

From a methodological perspective, such a study could be strengthened by the use of non-exchangeable $\delta^{2}H$ as an additional tool to even better distinguish and quantify more sources in mixing models. This tool has been recently shown to be powerful for such purposes (Ferchiche et al., 2025). From a fundamental perspective, aggregating more datasets from other temperate rivers would allow testing the robustness of this typology and probably detecting additional types, but also datasets from polar and tropical rivers to perform an even more comprehensive study at a global climate scale. Clearly, the approach developed in the present study is transferable to other regions of the planet and used at broader spatial scales. In addition, a similar study dedicated to the estuarine systems would even increase our comprehensive understanding of the origin and fate of POM along the Land-Ocean Aquatic Continuum by complementing the present study dedicated to the River-Estuary Interface and those of Liénart et al. (2017, 2018) dedicated to the coastal systems.

Appendix

Toward a typology of river functioning: a comprehensive study of the particulate organic matter composition at the multi-river scale

Florian Ferchiche[1], Camilla Liénart[1], Karine Charlier[1], Jonathan Deborde[2,3], Mélanie Giraud[4], Philippe Kerhervé[5], Pierre Polsenaere[1,3], Nicolas Savoye[1*]

[1] Univ. Bordeaux, CNRS, EPHE, Bordeaux INP, UMR 5805 EPOC, F-33600 Pessac, France

[2] Univ. Pau & Pays Adour, CNRS, E2S UPPA – MIRA, UMR 5254 IPREM, F-64000 Pau, F-64600 Anglet, France

[3] Ifremer, COAST, F-17390 La Tremblade, France

[4] MNHN~~, CRESCO~~, Station Marine de Dinard, F-35800 Dinard, France

[5] Univ. Perpignan, CNRS, UMR 5110 CEFREM, F-66860 Perpignan, France

*Correspondence to: Nicolas Savoye (nicolas.savoye@u-bordeaux.fr) (+33)556223916
Université de Bordeaux - UMR 5805 EPOC - Station marine d'Arcachon - 2 rue du Professeur Jolyet - 33120 Arcachon

*Corresponding author
nicolas.savoye@u-bordeaux.fr
Station marine - 2 rue du Professeur Jolyet 33120 ARCACHON

Keywords : River-Estuary Interface; particulate organic matter; isotopes; multi-ecosystem study

Table A1 Summary of data availability and origin (X means that the data were available; * means that the data were retrieved from the Naïades database; ** means that the data were retrieved from the Météo France database). n = number of sampling dates; SPM = Suspended Particulate Matter; POC or PN = Particulate Organic Carbon or Nitrogen; Chl *a* = Chlorophyll *a*; Phaeo = Phaeopigments.

River	Samplings					Parameters																			
	Dates	Periodicity	n	Latitude	Longitude	$\delta^{13}C$	$\delta^{15}N$	C/N ratio	SPM	POC	PN	Chl *a*	Phaeo	Water temperature	pH	Conductivity	NH_4^+	NO_2^-	NO_3^-	PO_4^{3-}	Flow	Rainfall	Air temperature	Wind direction	Wind intensity	Irradiance
Seine	06/2014 to 06/2015	monthly	13	49.306667	1.242500	X	X	X	X*	X	X	X	X	X*	X*	X*	X*	X*	X*	X*	X	X**	X**	X**	X**	
Orne	06/2014 to 06/2015	monthly	13	49.179722	-0.349167	X	X	X	X*	X	X	X	X	X*	X*	X*	X*	X*	X*	X*	X	X**	X**	X**	X**	X**
Rance	06/2014 to 05/2015	monthly	12	48.491667	-2.001389	X	X	X	X*	X	X	X	X	X*	X*	X*	X*	X*	X*	X*	X	X**	X**	X**	X**	X**
Elorn	01/2014 to 06/2015	monthly	17	48.450556	-4.248333	X	X	X	X*	X	X	X	X	X*	X*	X*	X*	X*	X*	X*	X	X**	X**	X**	X**	X**
Aulne	01/2014 to 06/2015	monthly	17	48.212778	-4.094444	X	X	X	X*	X	X	X	X	X*	X*	X*	X*	X*	X*	X*	X	X**	X**	X**	X**	X**
Loire	10/2009 to 07/2012	bi-monthly	67	47.392095	-0.860351	X	X	X	X*	X	X	X	X	X	X	X	X	X	X	X	X	X**	X**	X**	X**	X**
Sèvre niortaise	03/2014 to 03/2015	monthly	13	46.315348	-1.003891	X	X	X	X*	X	X	X	X	X*	X*	X*	X*	X*	X*	X*	X	X**	X**			
Charente	03/2014 to 03/2015	monthly	13	45.868056	-0.713056	X	X	X	X*	X	X	X	X	X*	X*	X*	X*	X*	X*		X	X**	X**	X**	X**	
Seudre	03/2014 to 09/2015	monthly	15	45.674027	-0.933123	X	X	X	X*	X	X	X	X	X*	X*	X*	X*	X*	X*	X*	X	X**	X**	X**	X**	X**
Porge	01/2008 to 02/2009	monthly	14	44.789868	-1.161181	X		X	X	X		X	X	X		X			X*		X	X**	X**	X**	X**	
Renet	02/2008 to 02/2009	bi-monthly	23	44.714466	-1.044013	X		X	X	X		X	X	X		X			X*		X	X**	X**	X**	X**	
Milieu	02/2008 to 02/2009	monthly	13	44.697326	-1.022532	X		X	X	X		X	X	X		X			X*		X	X**	X**	X**	X**	
Cirès	02/2008 to 02/2009	monthly	13	44.759820	-1.110657	X		X	X	X		X	X	X		X			X*		X	X**	X**	X**	X**	
Lanton	02/2008 to 02/2009	monthly	13	44.700283	-1.024385	X		X	X	X		X	X	X		X			X*		X	X**	X**	X**	X**	
Tagon	02/2008 to 02/2009	bi-monthly	26	44.659049	-0.989050	X		X	X	X		X	X	X		X			X*		X	X**	X**	X**	X**	
Landes	02/2008 to 02/2009	monthly	12	44.616912	-1.109066	X		X	X	X		X	X	X		X			X*		X	X**	X**	X**	X**	
Leyre	02/2008 to 02/2015	bi-monthly or monthly	59	44.626389	-0.996111	X	X	X	X*	X	X	X	X	X	X*	X*	X*	X*	X*	X*	X	X**	X**	X**	X**	
Adour	04/2013 to 05/2018	monthly	24	43.498880	-1.294899	X	X	X	X	X	X	X	X	X			X	X	X		X	X**	X**	X**	X**	X**
Têt	01/2006 to 05/2010	monthly	52	42.713704	2.993488	X	X	X	X	X	X			X	X	X	X*	X*	X*	X*	X	X**	X**	X**	X**	
Aude	01/2006 to 05/2010	monthly	52	43.244281	3.152733	X	X	X	X	X	X			X	X	X	X*	X*	X*	X*	X	X**	X**	X**	X**	X**
Orb	01/2006 to 05/2010	monthly	52	43.285004	3.281278	X	X	X	X	X	X			X	X	X	X*	X*	X*	X*	X	X**	X**			
Hérault	01/2006 to 05/2010	monthly	52	43.359415	3.435398	X	X	X	X	X	X			X	X	X	X*	X*	X*	X*	X	X**	X**	X**	X**	
Rhône	12/2003 to 01/2011	monthly	105	43.678724	4.621188	X	X	X	X	X	X	X	X	X	X	X	X*	X*	X*	X*	X	X**	X**	X**	X**	X**

River	SPM (mg/l)	Chlorophyll *a* (µg/l)	Phaeopigments (µg/l)	Temperature (°C)	River flow (m^3/s)	pH (unit)	Ammonium (µM)	Nitrates (µM)	Phosphates (µM)	Irradiance (j/m^2)	Zonal wind (m/s)	Meridional wind (m/s)
Seine	X	X	X	X	X	X	X	-	-		-	-
Orne	-	X	-	X	X	X	-	X	X	-	X	-
Rance	X	X	-	X	X	-	-	X	-	-	-	-
Elorn	-	X	X	-	X	-	X	-	X	-	-	-
Aulne	X	X	-	-	X	X	-	X	-	-	-	-
Sèvre	X	X	X	-	-	X	-	-	-			
Charente	-	X	X	-	X	X	-	-			-	X
Seudre	X	X	X	X	X	-	-	-	-	X	X	X
Porge	X	X	X	-	-						X	X
Cirès	X	X	X	X	X						-	-
Milieu	X	X	X	-	X						-	X
Lanton	X	X	X	X	-						-	X
Renet	X	X	X	X	-						-	-
Tagon	X	X	X	X	X						-	-
Leyre	X	X	X	X	-	X	-		-		-	-
Landes	X	X	X	-	X						-	X
Adour	X	-	X	X	X		X	-		-	-	-
Têt	X			X	X	X	-	X	-		-	X
Aude	X			X	X	-	X	-	X	X	-	-
Orb	X			X	X	X	-	X	X		-	-
Hérault	X			X	X	-	-	-	X	-	-	X
Rhône	X			-	X	-				-	-	-

X = Kept = No data

- = Non kept = Auto-correlated

Table A2 Summary of parameters kept (informative) to perform the local seasonal RDAs, opposite to those not considered (because non-informative, not available, or auto-correlated (see section 2.5)).

River	SPM	Chlorophyll *a*	Phaeopigments	Temperature	River flow	pH	Ammonium	Nitrates	Phosphates	Irradiance	Zonal wind	Meridional wind
Seine	X	X	X	X	X	X	X	-	-		-	-
Orne	-	X	-	X	X	X	-	X	X	-	X	-
Rance	X	X	-	X	X	-	-	X	-	-	-	-
Elorn	-	X	X	-	X	-	X	-	X	-	-	-
Aulne	X	X	-	-	X	X	-	X	-	-	-	-
Sèvre	X	X	X	-	-	X	-	-	-			
Charente	-	X	X	-	X	X	-	-			-	X
Seudre	X	X	X	X	X	-	-	-	-	X	X	X
Porge	X	X	X	-	-						X	X
Cirès	X	X	X	X	X						-	-
Milieu	X	X	X	-	X						-	X
Lanton	X	X	X	X	-						-	X
Renet	X	X	X	X	-						-	-
Tagon	X	X	X	X	X						-	-
Leyre	X	X	X	X	-	X	-		-		-	-
Landes	X	X	X	-	X						-	X
Adour	X	-	X	X	X		X	-		-	-	-
Têt	X			X	X	X	-	X	-		-	X
Aude	X			X	X	-	X	-	X	X	-	-
Orb	X			X	X	X	-	X	X		-	-
Hérault	X			X	X	-	-	-	X	-	-	X
Rhône	X			-	X	-				-	-	-

X = Kept = No data

- = Non kept = Auto-correlated

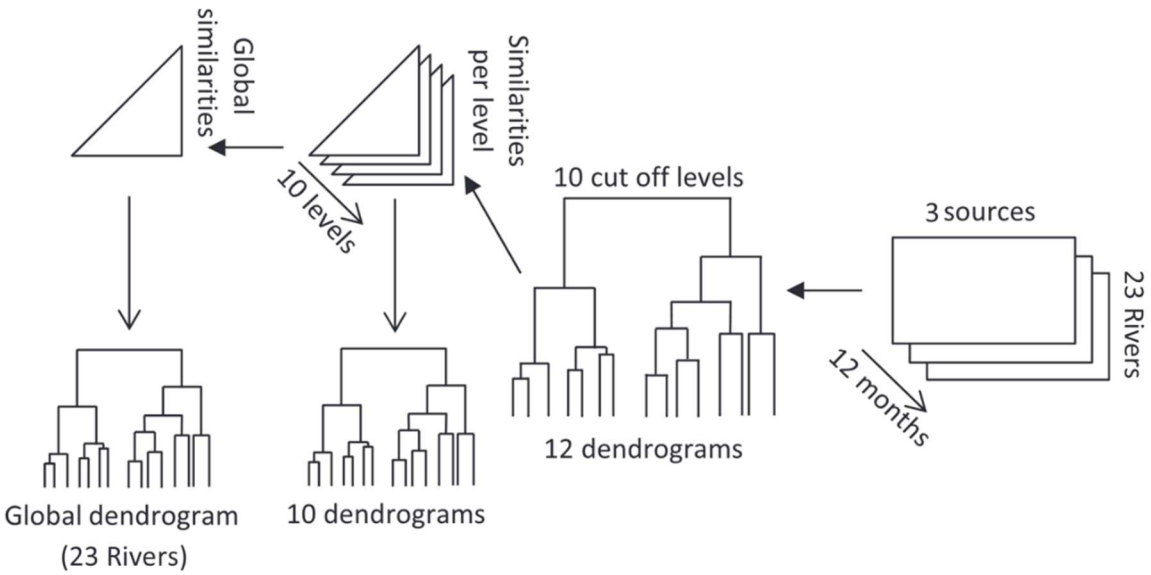

Figure A1 Diagram detailing the regionalisation method, adapted from Souissi et al. (2000).

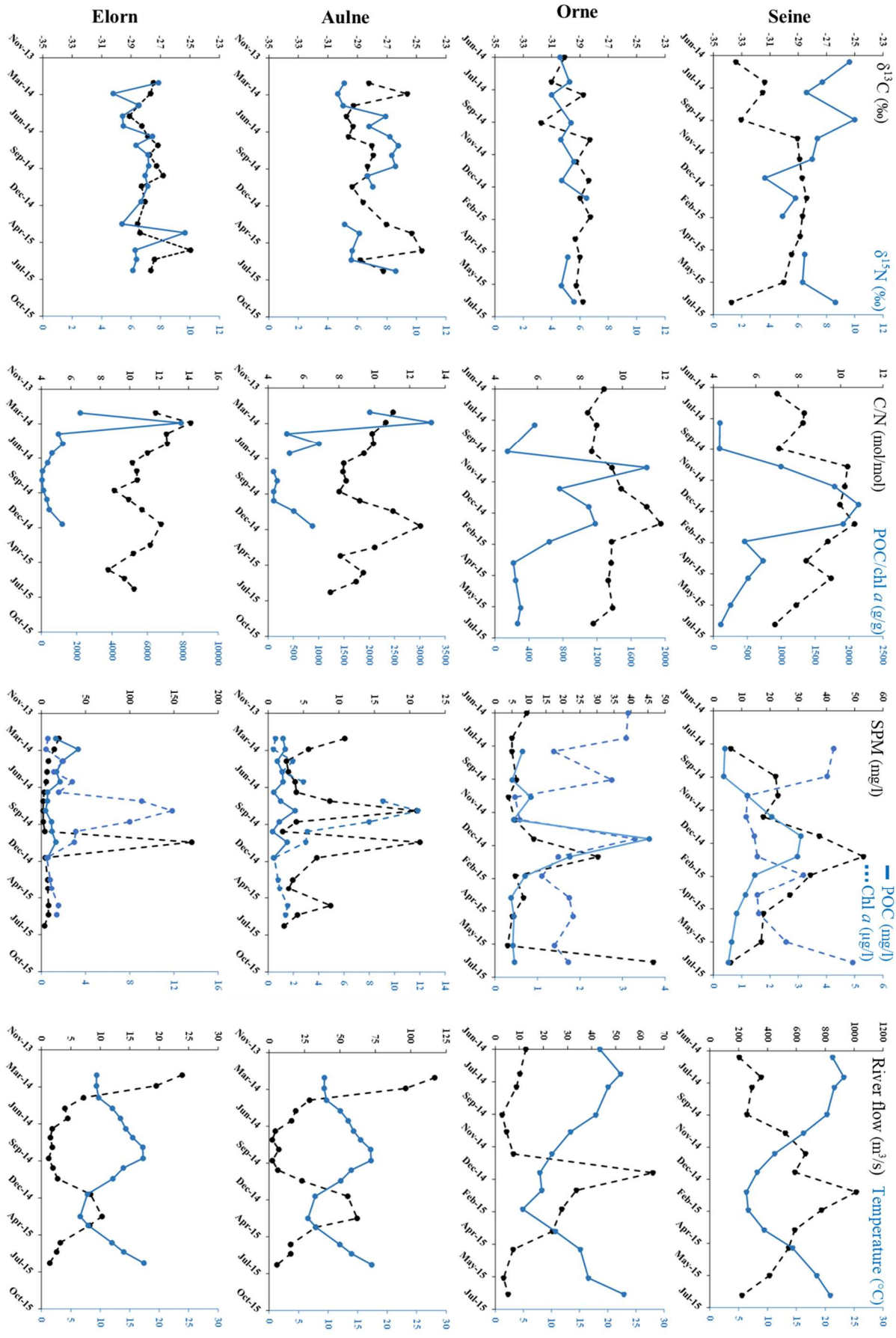
Seine
Orne
Aulne
Elorn
δ13C (‰)
δ15N (‰)
C/N (mol/mol)
POC/chl a (g/g)
SPM (mg/l)
POC (mg/l)
Chl a (µg/l)
River flow (m3/s)
Temperature (°C)

773

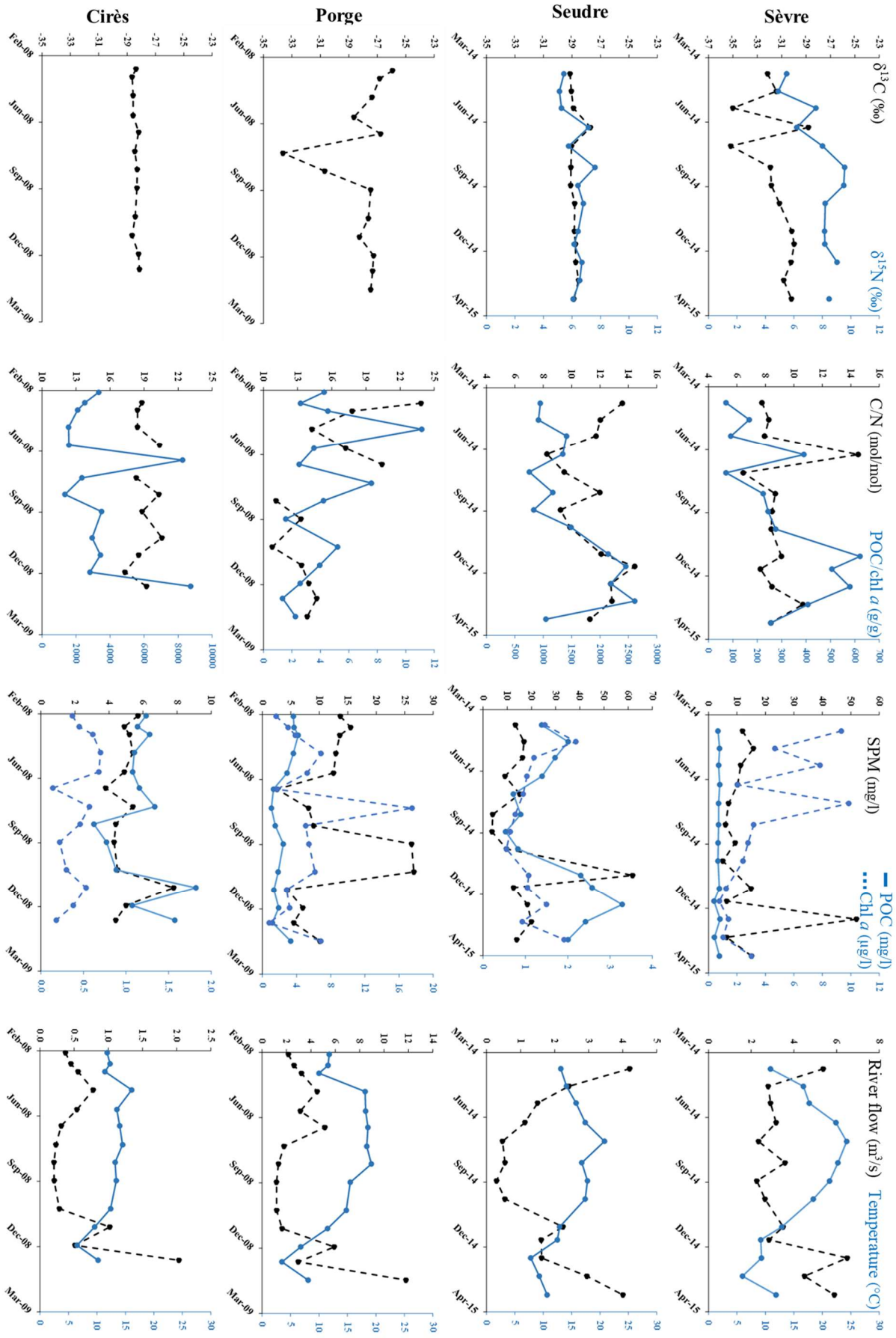
Sèvre
Seudre
Porge
Cirès
δ13C (‰)
δ15N (‰)
C/N (mol/mol)
POC/chl a (g/g)
SPM (mg/l)
POC (mg/l)
Chl a (µg/l)
River flow (m3/s)
Temperature (°C)
Mar-14
Jun-14
Sep-14
Dec-14
Apr-15
Feb-08
Jun-08
Sep-08
Dec-08
Mar-09

774

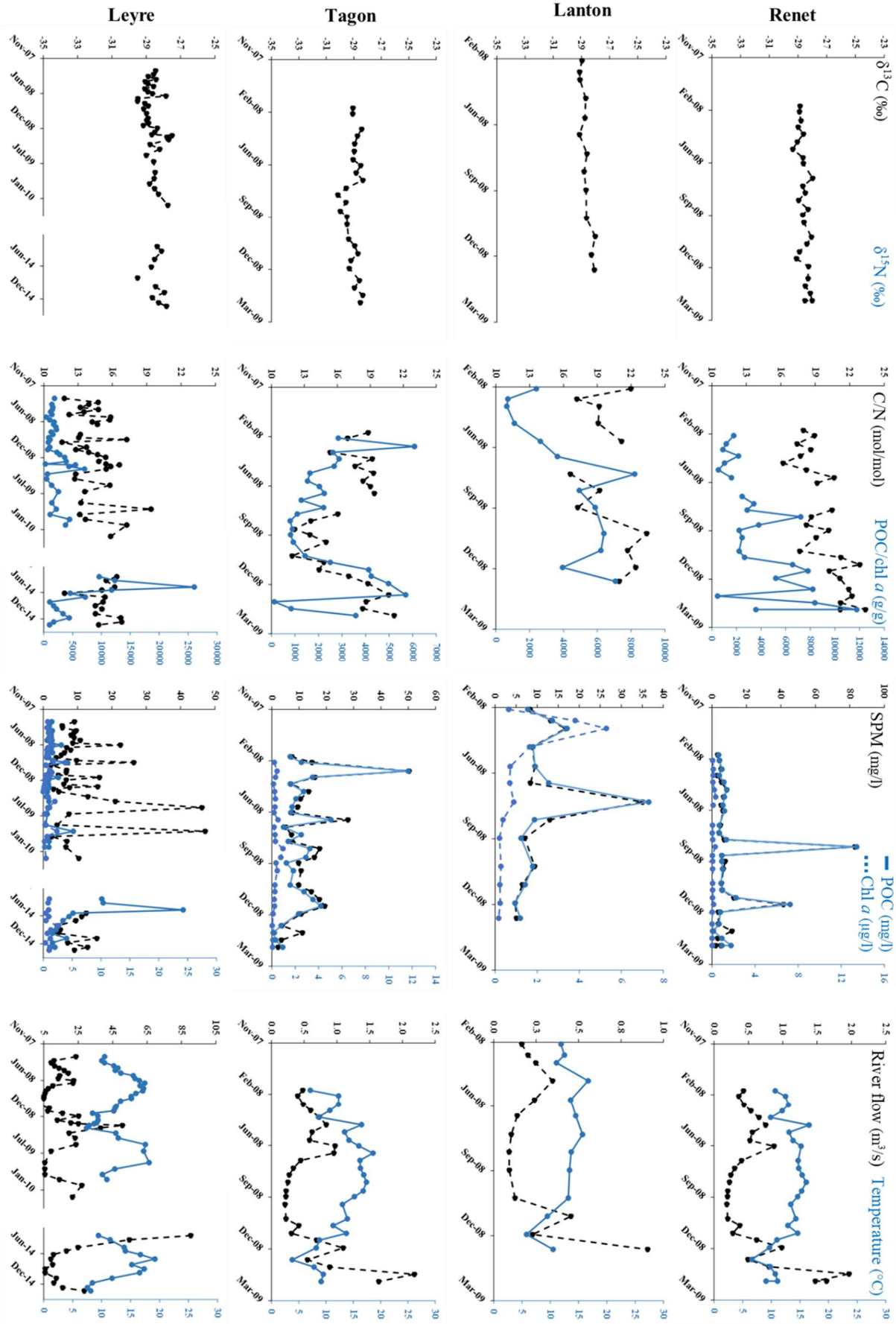
Renet
Lanton
Tagon
Leyre
δ13C (‰)
δ15N (‰)
C/N (mol/mol)
POC/chl a (g/g)
SPM (mg/l)
POC (mg/l)
Chl a (µg/l)
River flow (m3/s)
Temperature (°C)

775

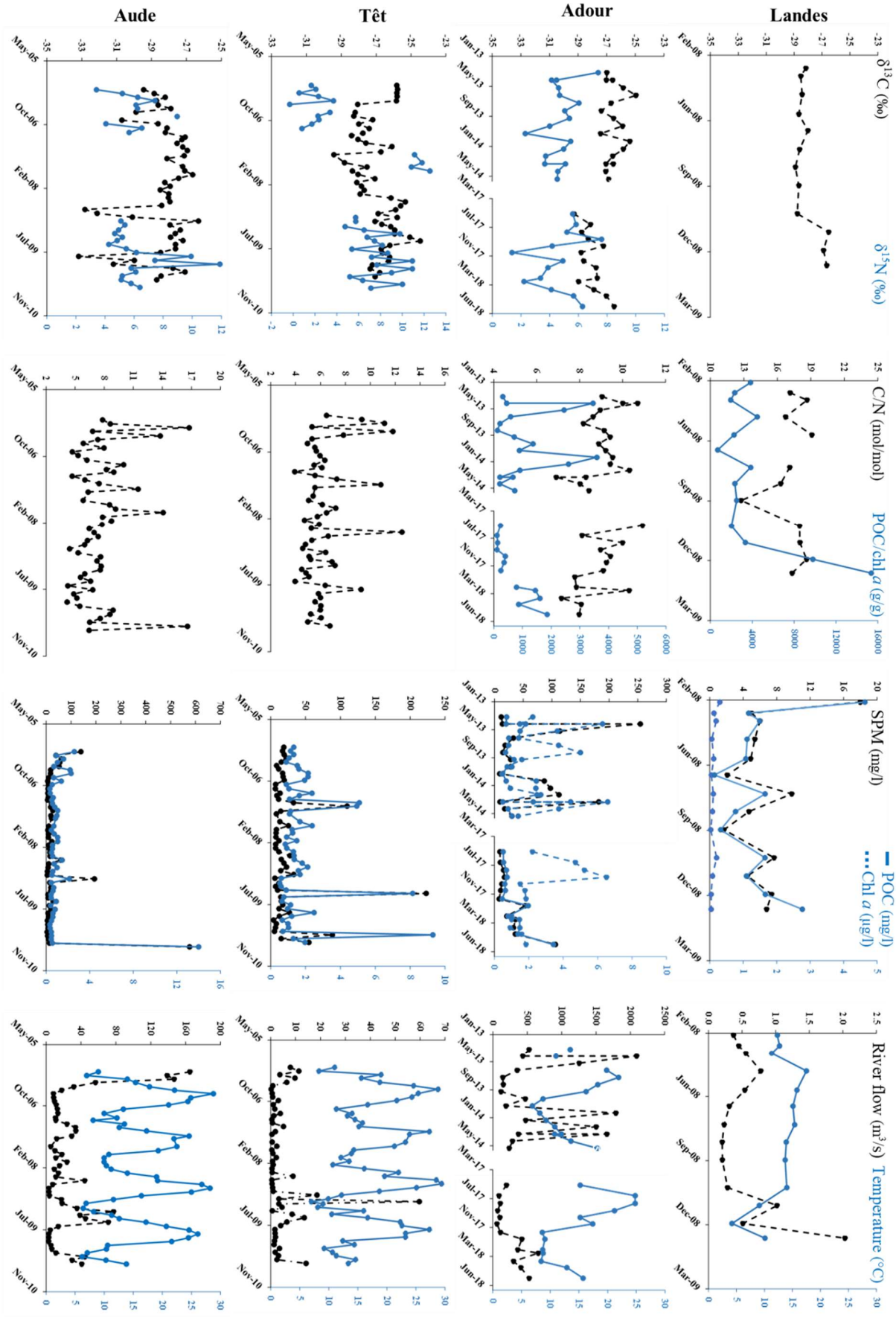
Landes
Adour
Têt
Aude
δ13C (‰)
δ15N (‰)
C/N (mol/mol)
POC/chl a (g/g)
SPM (mg/l)
POC (mg/l)
Chl a (µg/l)
River flow (m3/s)
Temperature (°C)

776

777

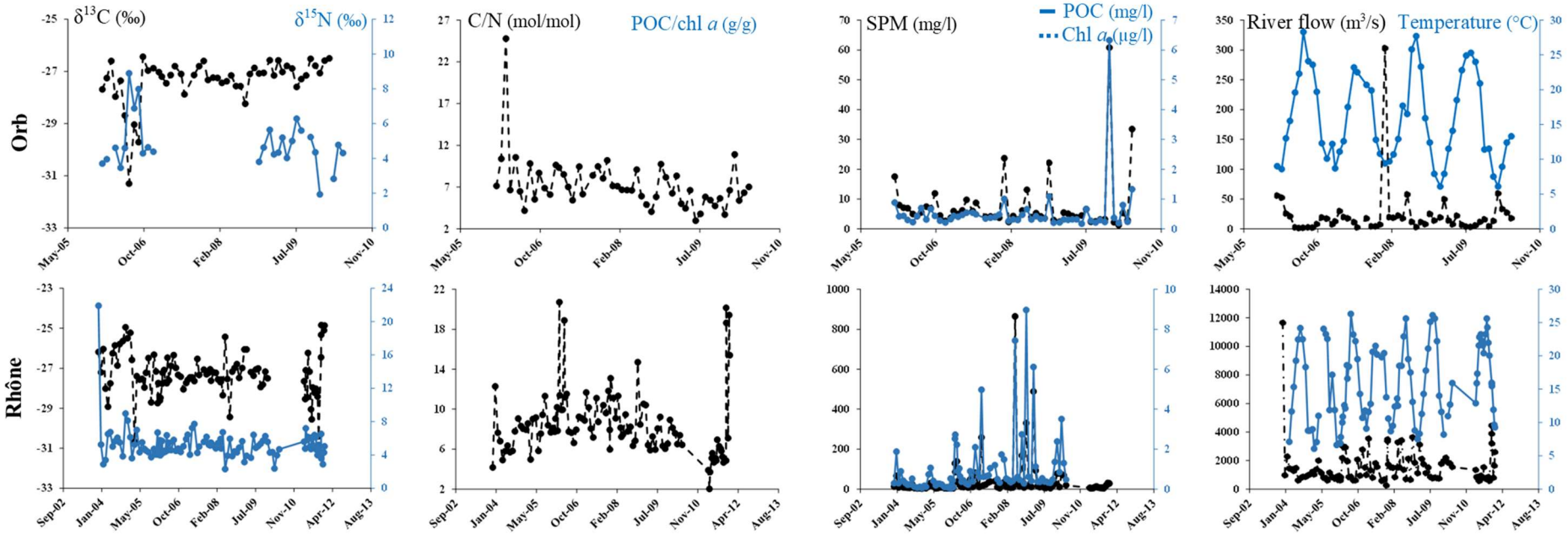

Figure A2 Temporal variations of matter characteristics for representative rivers along the studied periods for $\delta^{13}C$ (left axis; black dotted line) and $\delta^{15}N$ (right axis; blue line) (first column); C/N (left axis; black dotted line) and POC/chl a(right axis; blue line) ratios (second column); SPM(left axis; black dotted line), POC (right axis; blue line) and chlorophyll *a* (right axis; blue dotted line) concentrations (third column) and river flow (left axis; black dotted line) and temperature (right axis; blue line) (fourth column).

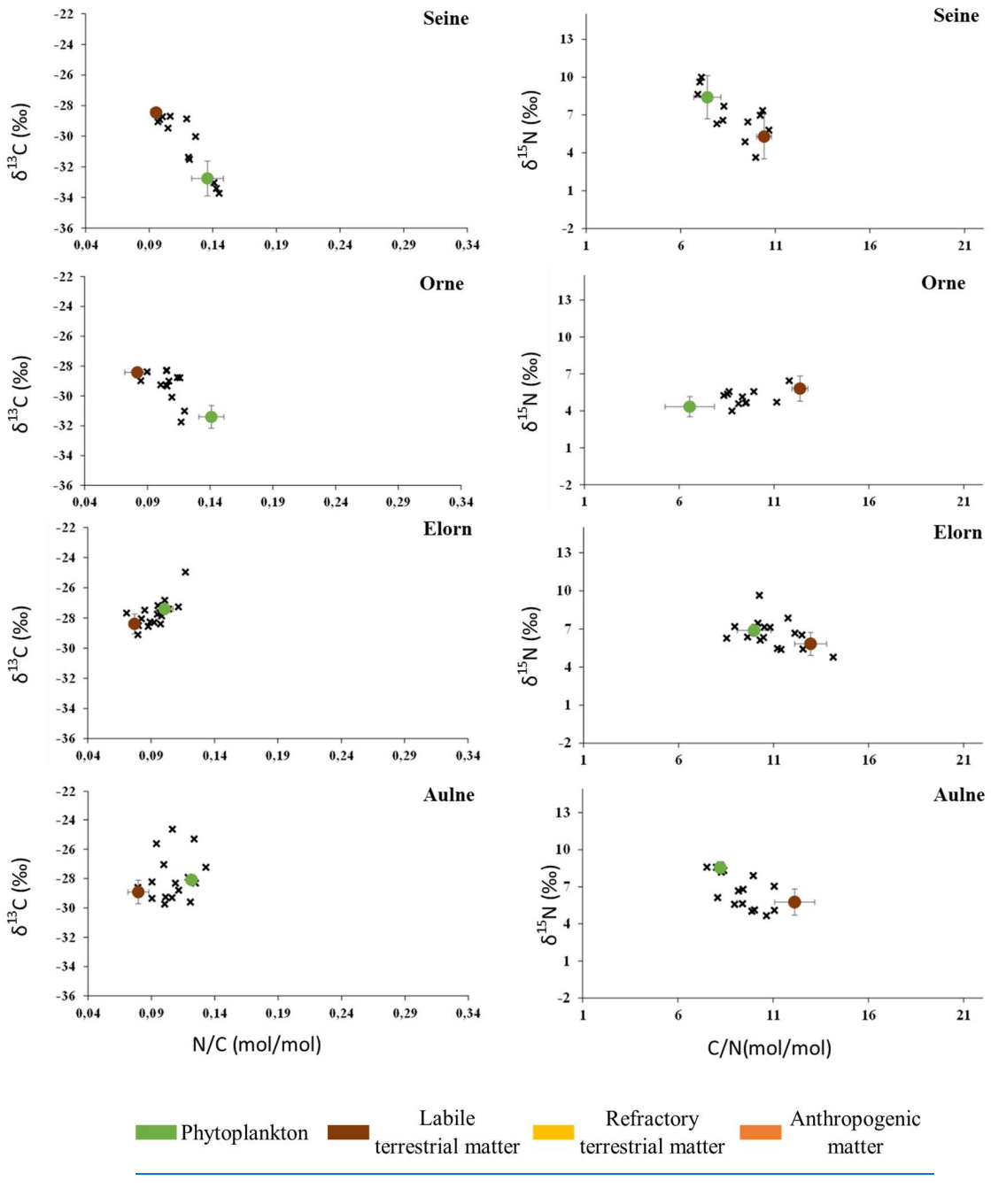
Seine
Orne
Elorn
Aulne
δ13C (‰)
δ15N (‰)
N/C (mol/mol)
C/N(mol/mol)
Phytoplankton
Labile terrestrial matter
Refractory terrestrial matter
Anthropogenic matter

779

780

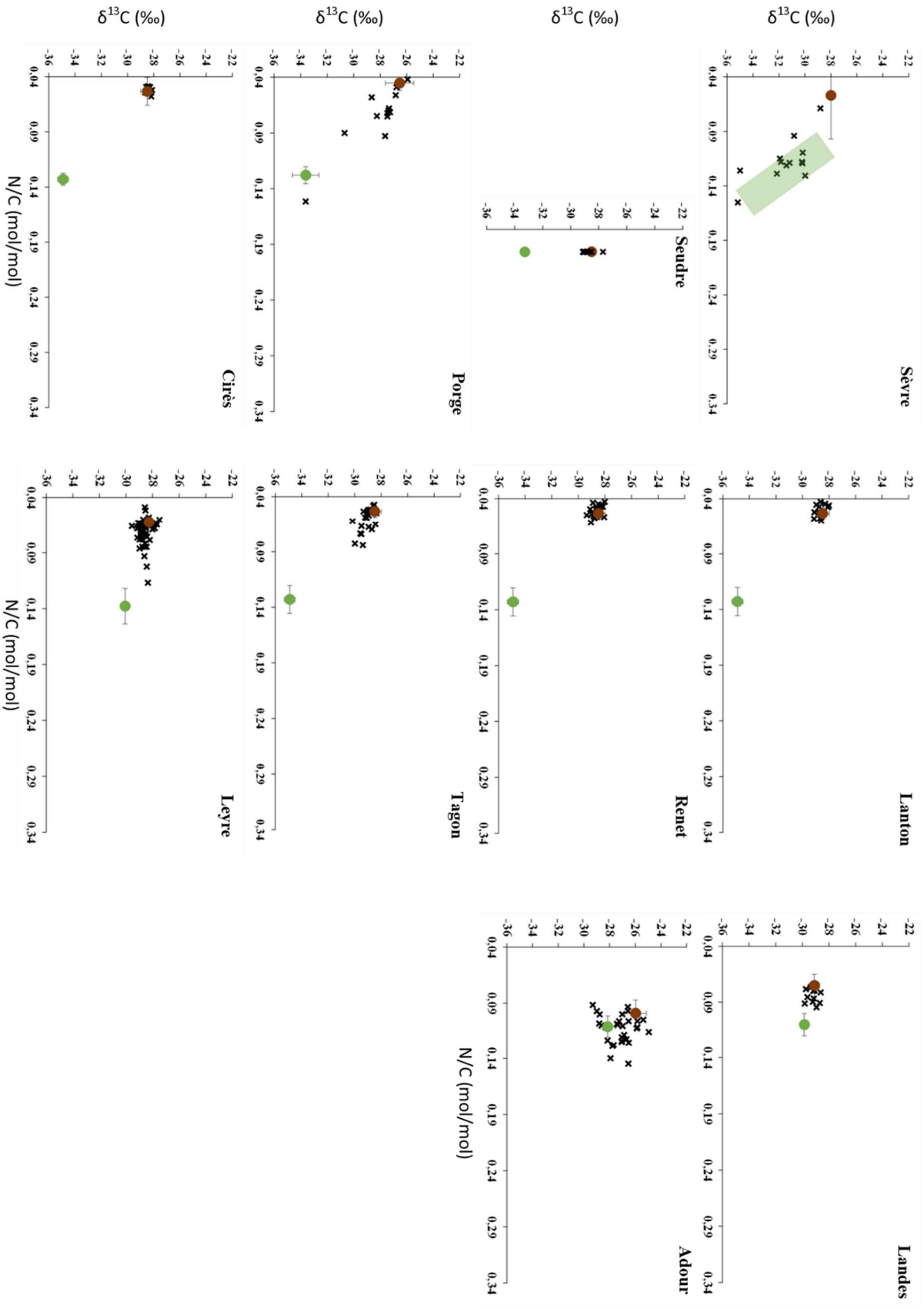
δ13C (‰)
N/C (mol/mol)
Sèvre
Lanton
Landes
Seudre
Renet
Adour
Porge
Tagon
Cirès
Leyre

781

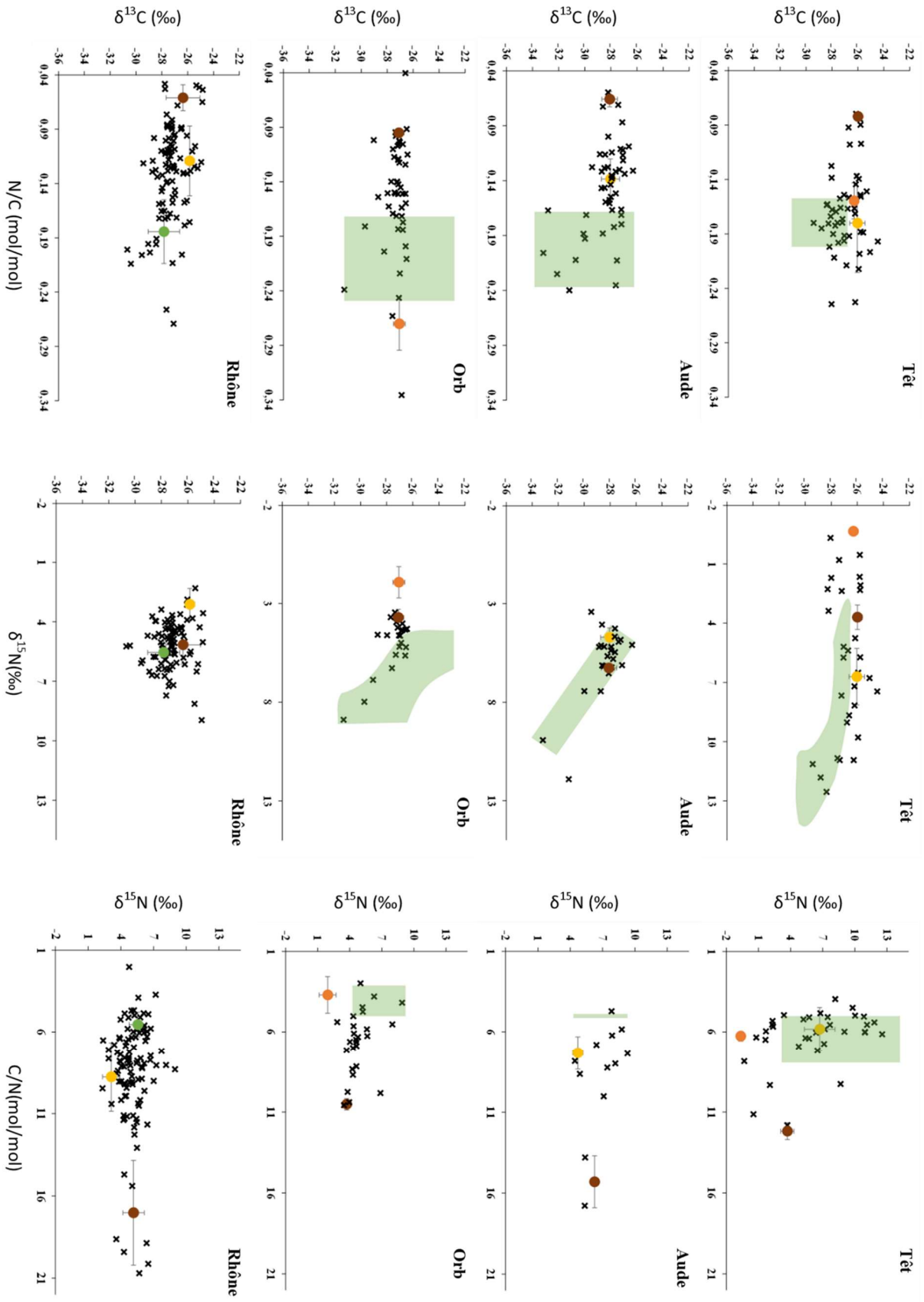

782

783 Figure A3 $\delta^{13}C$, $\delta^{15}N$, N/C and/or C/N values of bulk POM (black crosses) and sources. The
784 latter are presented as closed circles (average) and bars (standard deviation) when the signatures

were constant over time and by colored area when at least one of the proxies was variable over time (see Table 2). This colored area corresponds to the dispersion of the values, including their uncertainties.

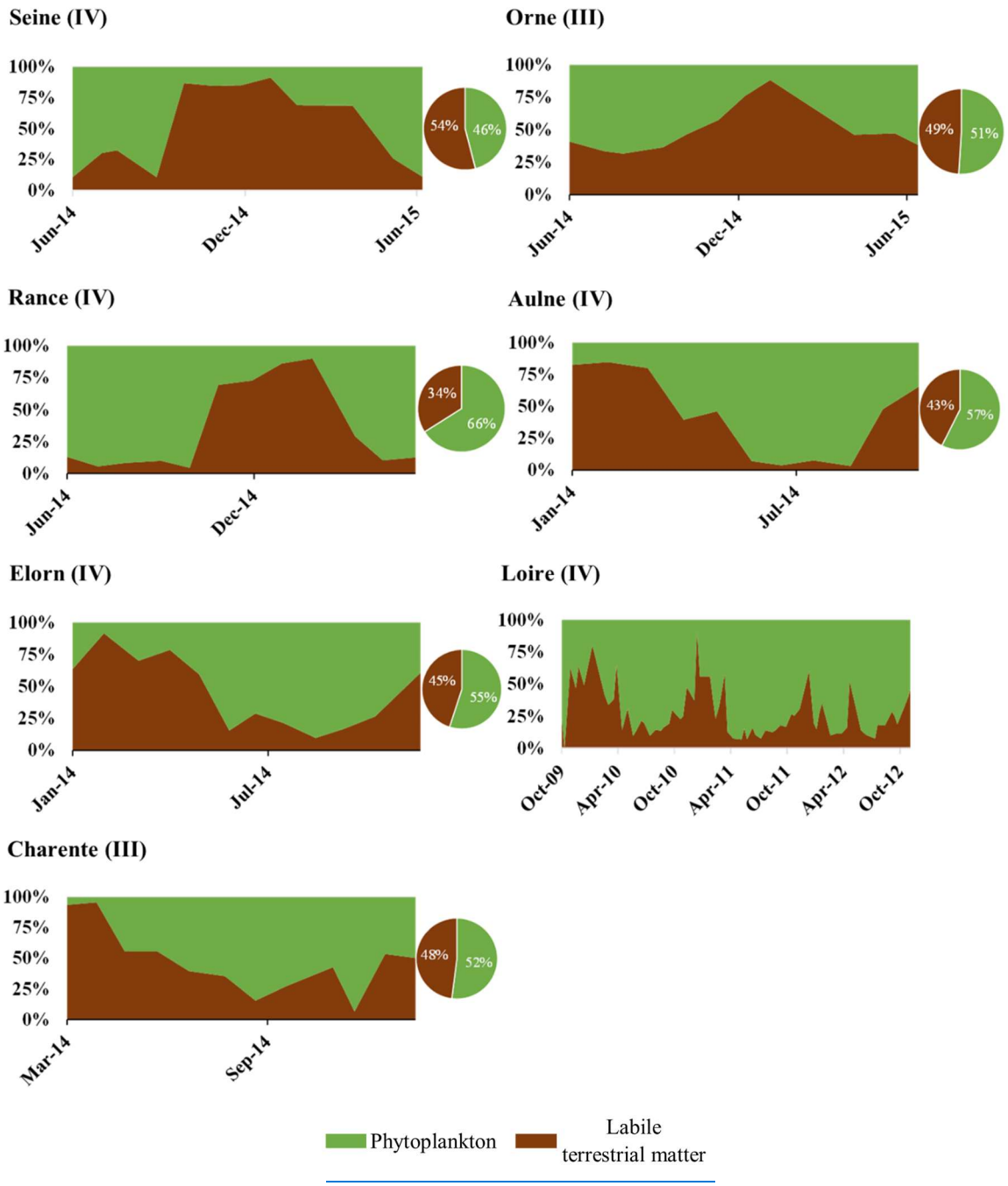

Figure A4 Temporal dynamic (rectangle graphs) and (inter-)annual mean (pie charts) of PN source proportions. Sources are phytoplankton (green) and labile terrestrial material (brown).

Tagon (I)

Adj. R^2 0.70

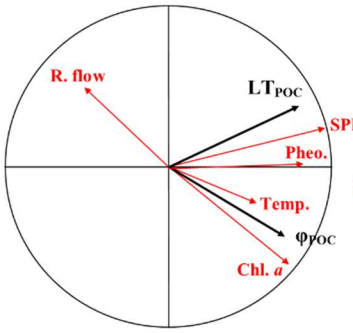

Lanton (I)

Adj. R^2 0.93

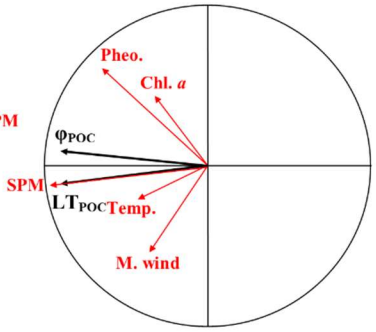

Leyre (I)

Adj. R^2 0.41

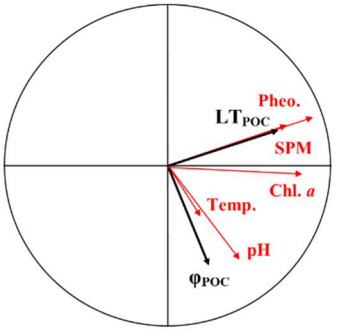

Cirès (I)

Adj. R^2 0.74

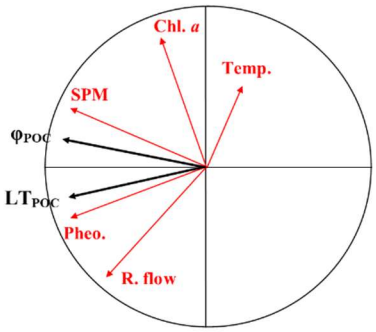

Renet (I)

Adj. R^2 0.97

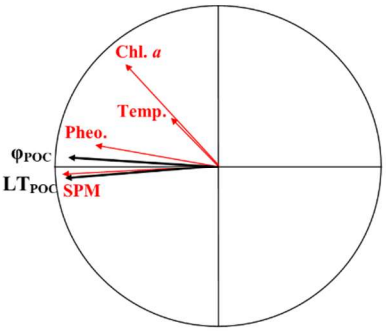

Seudre (I)

Adj. R^2 0.74

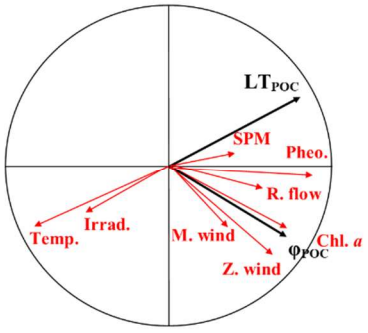

Porge (II)

Adj. R^2 0.38

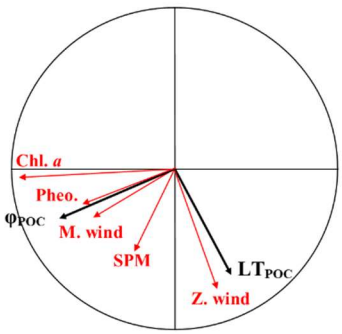

Adour (II)

Adj. R^2 0.53

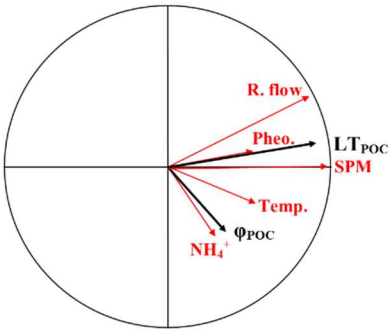

Landes (II)

Adj. R^2 0.61

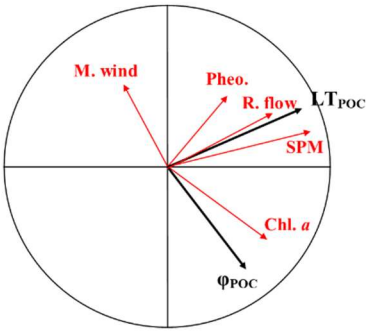

Orne C (II)

Adj. R^2 0.72

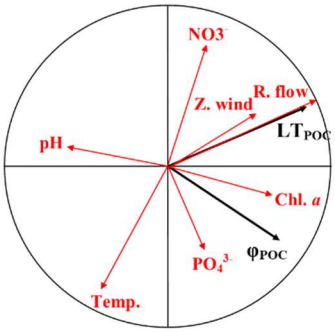

Orne N (II)

Adj. R^2 0.74

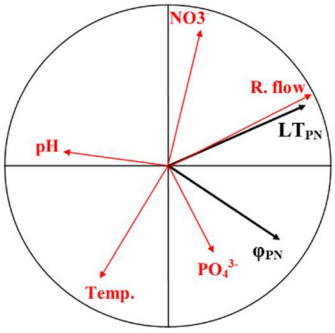

Charente N (II)

Adj. R^2 0.43

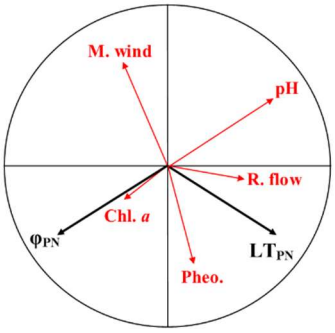

793

794

795

796

797

798

Seine C (IV)

Adj. R^2 0.95

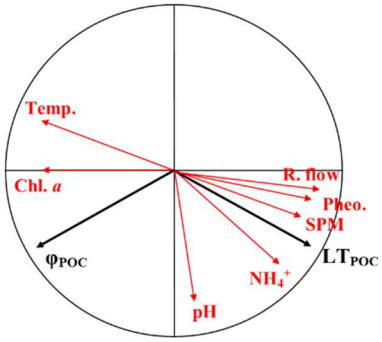

Aulne C (IV)

Adj. R^2 0.92

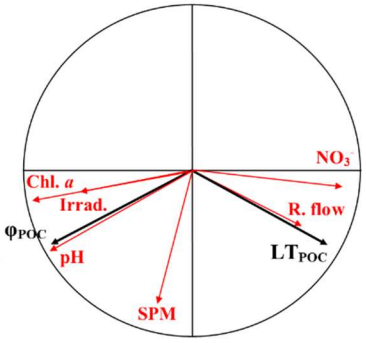

Elorn C (IV)

Adj. R^2 0.24

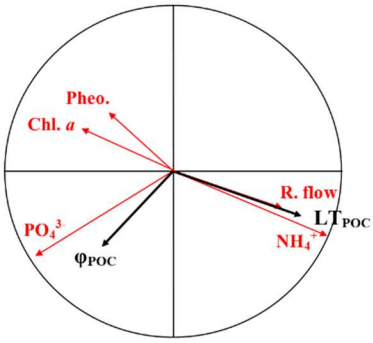

Seine N (IV)

Adj. R^2 0.80

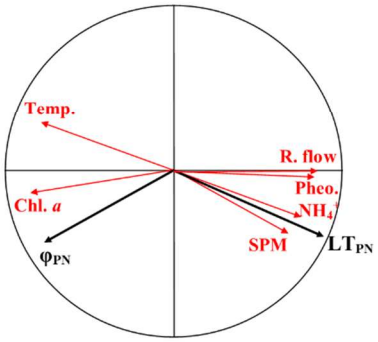

Aulne N (IV)

Adj. R^2 0.74

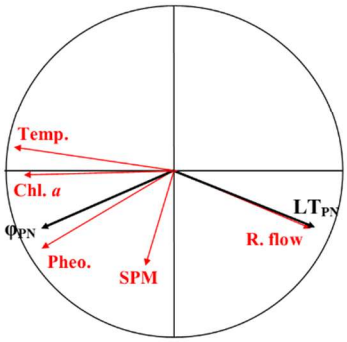

Elorn N (IV)

Adj. R^2 0.04

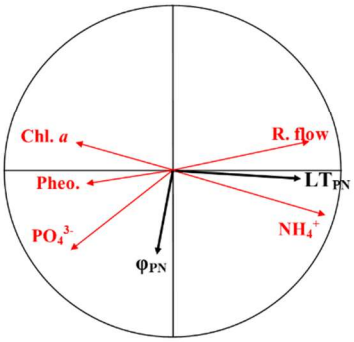

Rance N (IV)

Adj. R^2 0.56

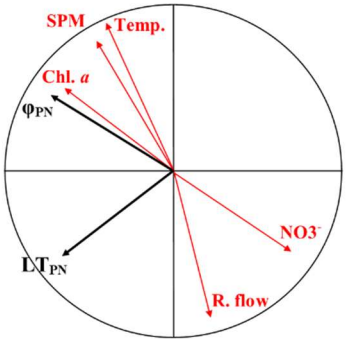

Sèvre (IV)

Adj. R^2 0.01

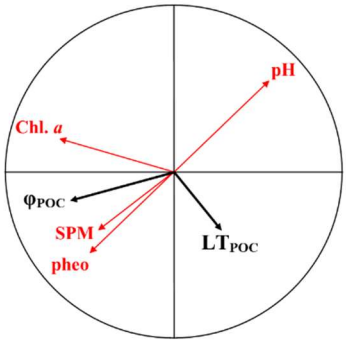

799

800

801

802

803

804

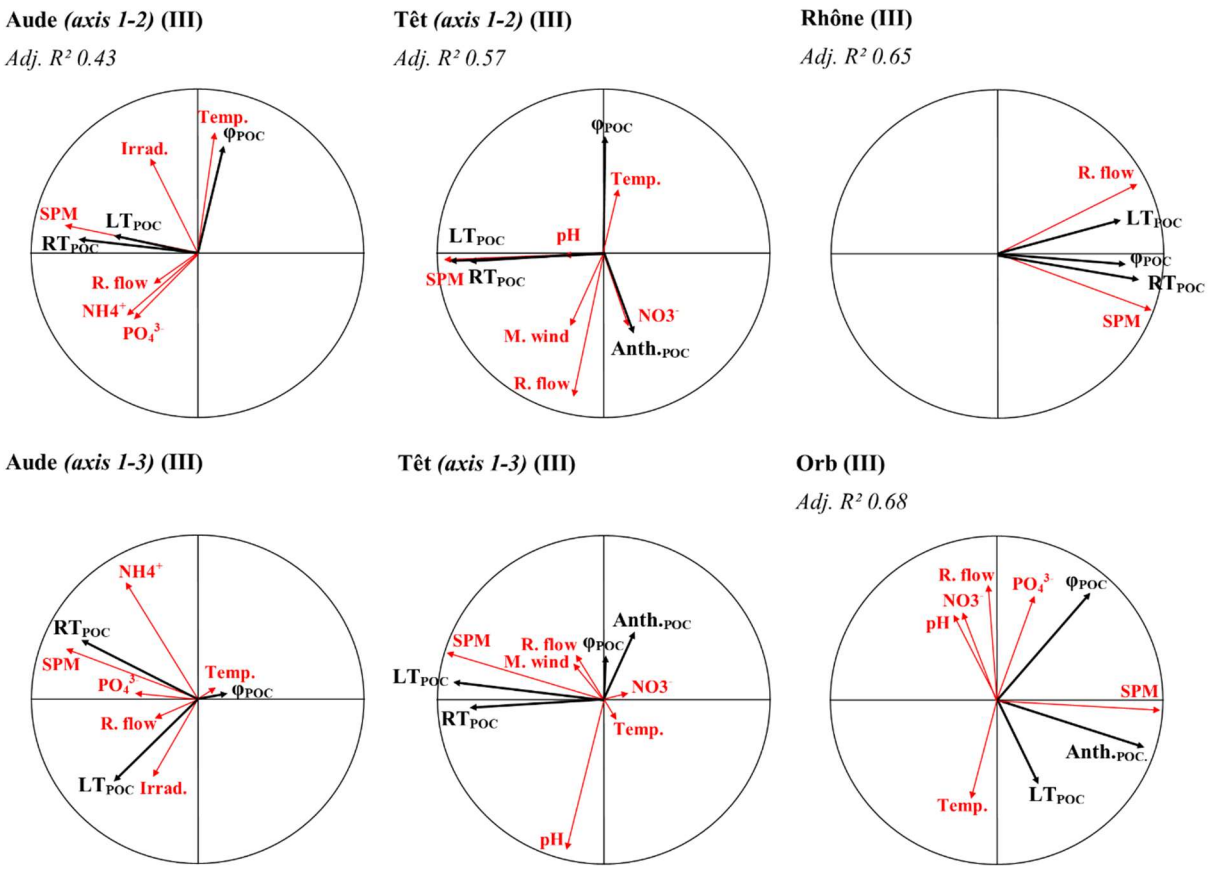

Figure A5 Redundancy analyses (correlation circles) of rivers standing for each type of river. Black arrows represent explained variables (concentration of POC or PN sources) and red arrows represent explaining variables (environmental variables). River types are recalled (Roman numerals). $LT_{POC\ or\ PN}$ = Labile terrestrial POC or PN; RT_{POC} = Refractory terrestrial POC; $\varphi_{POC\ or\ PN}$ = Phytoplankton POC or PN; Anth. POC = Anthropogenic POM; SPM = Suspended particulate matter; Chl *a* = chlorophyll a; Phaeo. = phaeopigments; M. wind = meridional wind; Z. wind = zonal wind; R. flow = river flow; Temp. = temperature; Irrad. = Irradiance; NH_4^+ = ammonium; NO_3^- = nitrate; PO_4^{3-} = phosphates; Adj. R^2 = adjusted R^2.

820

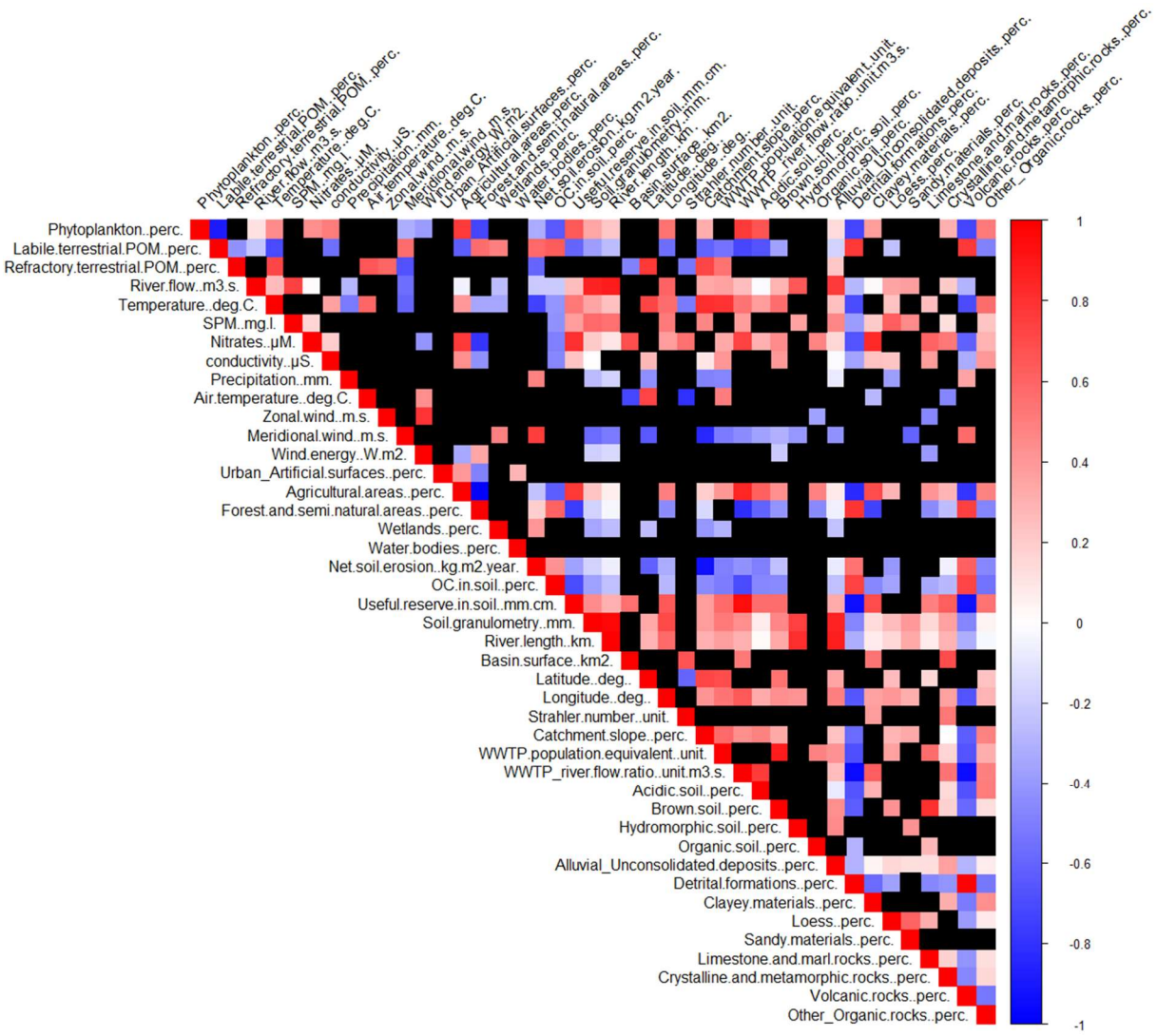
Phytoplankton..perc.
Labile.terrestrial.POM..perc.
Refractory.terrestrial.POM..perc.
River.flow..m3.s.
Temperature..deg.C.
SPM..mg.l.
Nitrates..µM.
conductivity..µS.
Precipitation..mm.
Air.temperature..deg.C.
Zonal.wind..m.s.
Meridional.wind..m.s.
Wind.energy..W.m2.
Urban_Artificial.surfaces..perc.
Agricultural.areas..perc.
Forest.and.semi.natural.areas..perc.
Wetlands..perc.
Water.bodies..perc.
Net.soil.erosion..kg.m2.year.
OC.in.soil..perc.
Useful.reserve.in.soil..mm.cm.
Soil.granulometry..mm.
River.length..km.
Basin.surface..km2.
Latitude..deg..
Longitude..deg..
Strahler.number..unit.
Catchment.slope..perc.
WWTP.population.equivalent..unit.
WWTP_river.flow.ratio..unit.m3.s.
Acidic.soil..perc.
Brown.soil..perc.
Hydromorphic.soil..perc.
Organic.soil..perc.
Alluvial_Unconsolidated.deposits..perc.
Detrital.formations..perc.
Clayey.materials..perc.
Loess..perc.
Sandy.materials..perc.
Limestone.and.marl.rocks..perc.
Crystalline.and.metamorphic.rocks..perc.
Volcanic.rocks..perc.
Other_Organic.rocks..perc.
1
0.8
0.6
0.4
0.2
0
-0.2
-0.4
-0.6
-0.8
-1

821

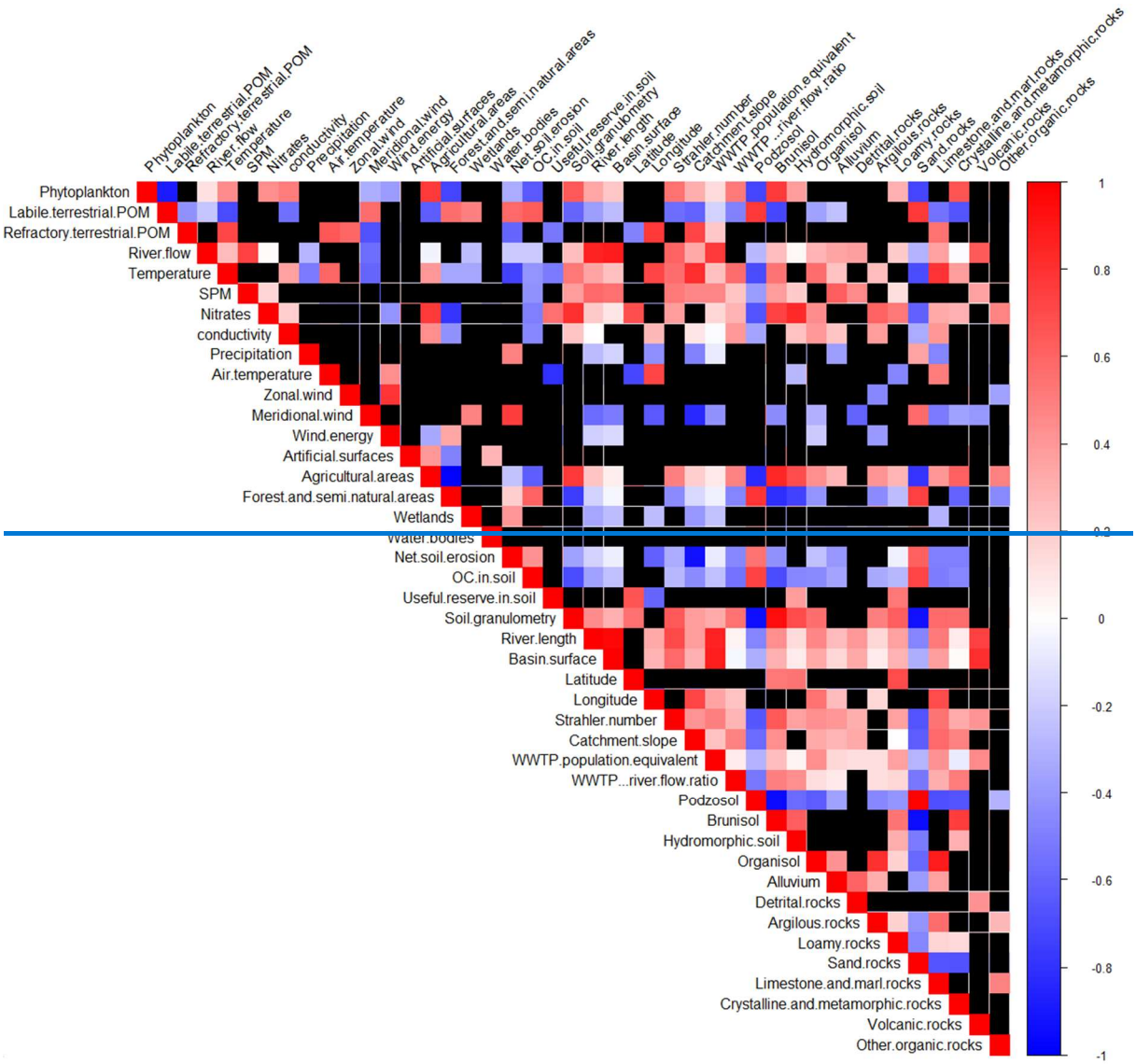

Figure A6 Correlogram of multi-system RDA parameters, including source proportions and accompanying parameters. Descriptions of environmental parameters can be retrieved in section 2.5. Temperature = Water temperature; SPM = Suspended particulate matter; OC in soil = Organic carbon proportions in soil; WWTP population equivalent = sewage treatment capacities; WWTP …River flow = sewage treatment capacities to average river flow ratio.

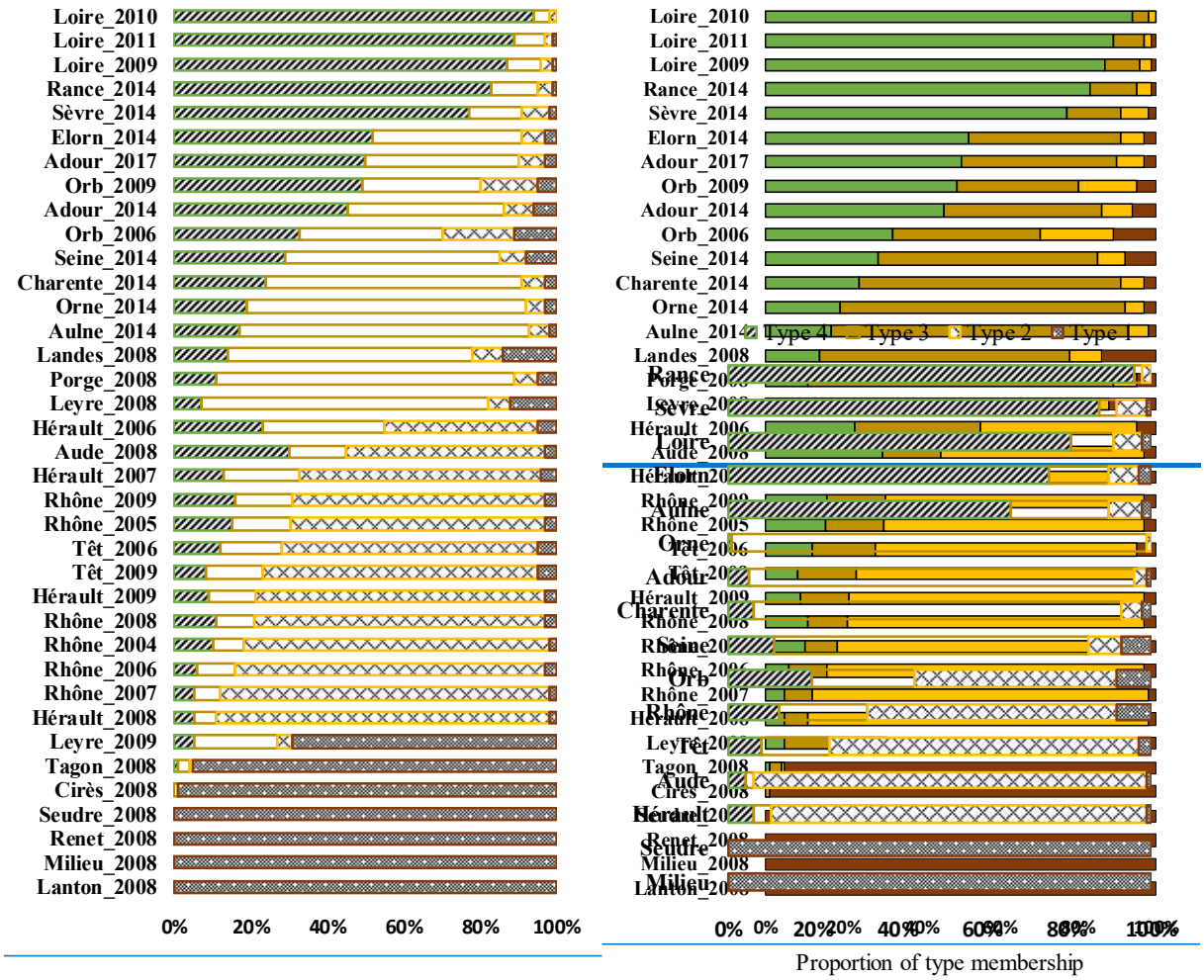
Loire_2010
Loire_2011
Loire_2009
Rance_2014
Sèvre_2014
Elorn_2014
Adour_2017
Orb_2009
Adour_2014
Orb_2006
Seine_2014
Charente_2014
Orne_2014
Aulne_2014
Landes_2008
Porge_2008
Leyre_2008
Hérault_2006
Aude_2008
Hérault_2007
Rhône_2009
Rhône_2005
Têt_2006
Têt_2009
Hérault_2009
Rhône_2008
Rhône_2004
Rhône_2006
Rhône_2007
Hérault_2008
Leyre_2009
Tagon_2008
Cirès_2008
Seudre_2008
Renet_2008
Milieu_2008
Lanton_2008
0%
20%
40%
60%
80%
100%
Type 4
Type 3
Type 2
Type 1
Proportion of type membership

832

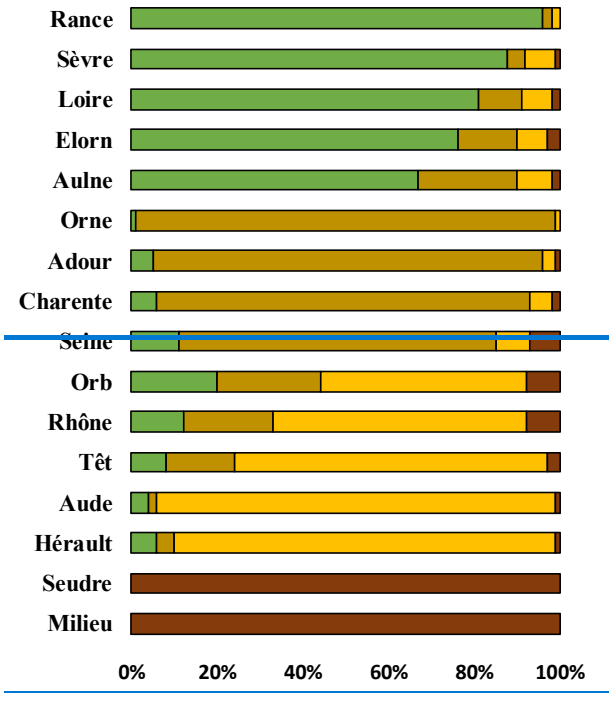
Rance
Sèvre
Loire
Elorn
Aulne
Orne
Adour
Charente
Seine
Orb
Rhône
Têt
Aude
Hérault
Seudre
Milieu
0%
20%
40%
60%
80%
100%

833

834

Figure A7 Typology of river dynamics following a hierarchical cluster analysis on POM source proportions. The percentages of membership for each type attributed to each river are shown. Left panel: considering all sampling years for all rivers. Right panel: considering only one stream of type I fuelling the Bay of Arcachon (Milieu River).

Author contributions

FF: Formal analysis, Investigation, Visualisation, Writing – original draft. CL: Formal analysis, Conceptualisation, Supervision, Writing – original draft, Writing – review & editing. KC: Investigation. JD: Investigation, Visualisation, Writing – review & editing. MG: Investigation. PK: Investigation. PP: Investigation, Visualisation, Writing – review & editing.

NS: Conceptualisation, Formal analysis, Investigation, Methodology, Supervision, Writing – original draft, Writing – review & editing.

Competing interest

The authors declare that they have no known competing financial interests or personal relationships that could have appeared to influence the work reported in this paper.

Data availability

All POM and environmental data used in this article are stored in Figshare, accessible for the review process through this private link : https://figshare.com/s/a7101028e6ab5452c4db.

References

Arellano, A. R., Bianchi, T. S., Osburn, C. L., D'Sa, E. J., Ward, N. D., Oviedo-Vargas, D., Joshi, I. D., Ko, D. S., Shields, M. R., Kurian, G., and Green, J.: Mechanisms of Organic Matter Export in Estuaries with Contrasting Carbon Sources, Journal of Geophysical Research: Biogeosciences, 124, 3168–3188, https://doi.org/10.1029/2018JG004868, 2019.

Barros, G. V., Martinelli, L. A., Oliveira Novais, T. M., Ometto, J. P. H. B., and Zuppi, G. M.: Stable isotopes of bulk organic matter to trace carbon and nitrogen dynamics in an estuarine ecosystem in Babitonga Bay (Santa Catarina, Brazil), Science of The Total Environment, 408, 2226–2232, https://doi.org/10.1016/j.scitotenv.2010.01.060, 2010.

Bate, G. C., Whitfield, A. K., Adams, J. B., Huizinga, P., and Wooldridge, T. H.: The importance of the river-estuary interface (REI) zone in estuaries, Water SA, 28, 271–280, https://doi.org/10.4314/wsa.v28i3.4894, 2002.

Bonin, P., Prime, A.-H., Galeron, M.-A., Guasco, S., and Rontani, J.-F.: Enhanced biotic degradation of terrestrial POM in an estuarine salinity gradient: interactive effects of organic matter pools and changes of bacterial communities, Aquatic Microbial Ecology, 83, 147–159, https://doi.org/10.3354/ame01908, 2019.

875 Borcard, D., Legendre, P., and Gillet, F.: Numerical Ecology with R, Springer, 315 pp., 2011.

876 Bouwman, L., Beusen, A., Glibert, P. M., Overbeek, C., Pawlowski, M., Herrera, J., Mulsow,
877 S., Yu, R., and Zhou, M.: Mariculture: significant and expanding cause of coastal nutrient
878 enrichment, Environ. Res. Lett., 8, 044026, https://doi.org/10.1088/1748-9326/8/4/044026,
879 2013.

880 Brett, M. T., Bunn, S. E., Chandra, S., Galloway, A. W. E., Guo, F., Kainz, M. J., Kankaala,
881 P., Lau, D. C. P., Moulton, T. P., Power, M. E., Rasmussen, J. B., Taipale, S. J., Thorp, J. H.,
882 and Wehr, J. D.: How important are terrestrial organic carbon inputs for secondary production
883 in freshwater ecosystems?, Freshwater Biology, 62, 833–853,
884 https://doi.org/10.1111/fwb.12909, 2017.

885 Canton, M., Anschutz, P., Coynel, A., Polsenaere, P., Auby, I., and Poirier, D.: Nutrient
886 export to an Eastern Atlantic coastal zone: first modeling and nitrogen mass balance,
887 Biogeochemistry, 107, 361–377, https://doi.org/10.1007/s10533-010-9558-7, 2012.

888 Canuel, E. A. and Hardison, A. K.: Sources, Ages, and Alteration of Organic Matter in
889 Estuaries, Annual Review of Marine Science, 8, 409–434, https://doi.org/10.1146/annurev-
890 marine-122414-034058, 2016.

891 Cathalot, C., Rabouille, C., Tisnérat-Laborde, N., Toussaint, F., Kerhervé, P., Buscail, R.,
892 Loftis, K., Sun, M.-Y., Tronczynski, J., Azoury, S., Lansard, B., Treignier, C., Pastor, L., and
893 Tesi, T.: The fate of river organic carbon in coastal areas: A study in the Rhône River delta
894 using multiple isotopic (δ13C, Δ14C) and organic tracers, Geochimica et Cosmochimica
895 Acta, 118, 33–55, https://doi.org/10.1016/j.gca.2013.05.001, 2013.

896 Chevalier, N., Savoye, N., Dubois, S., Lama, M. L., David, V., Lecroart, P., le Ménach, K.,
897 and Budzinski, H.: Precise indices based on *n*-alkane distribution for quantifying sources of
898 sedimentary organic matter in coastal systems, Organic Geochemistry, 88, 69–77,
899 https://doi.org/10.1016/j.orggeochem.2015.07.006, 2015.

900 Copard, Y., Eyrolle, F., Radakovitch, O., Poirel, A., Raimbault, P., Gairoard, S., and Di-
901 Giovanni, C.: Badlands as a hot spot of petrogenic contribution to riverine particulate organic
902 carbon to the Gulf of Lion (NW Mediterranean Sea), Earth Surface Processes and Landforms,
903 43, 2495–2509, https://doi.org/10.1002/esp.4409, 2018.

904 Copard, Y., Eyrolle, F., Grosbois, C., Lepage, H., Ducros, L., Morereau, A., Bodereau, N.,
905 Cossonnet, C., and Desmet, M.: The unravelling of radiocarbon composition of organic
906 carbon in river sediments to document past anthropogenic impacts on river systems, Science
907 of The Total Environment, 806, 150890, https://doi.org/10.1016/j.scitotenv.2021.150890,
908 2022.

909 Dagg, M., Benner, R., Lohrenz, S., and Lawrence, D.: Transformation of dissolved and
910 particulate materials on continental shelves influenced by large rivers: plume processes,
911 Continental Shelf Research, 24, 833–858, https://doi.org/10.1016/j.csr.2004.02.003, 2004.

912 Dalzell, B. J., Filley, T. R., and Harbor, J. M.: The role of hydrology in annual organic carbon
913 loads and terrestrial organic matter export from a midwestern agricultural watershed,
914 Geochimica et Cosmochimica Acta, 71, 1448–1462,
915 https://doi.org/10.1016/j.gca.2006.12.009, 2007.

David, V., Sautour, B., Chardy, P., and Leconte, M.: Long-term changes of the zooplankton variability in a turbid environment: The Gironde estuary (France), Estuarine, Coastal and Shelf Science, 64, 171–184, https://doi.org/10.1016/j.ecss.2005.01.014, 2005.

Deborde, J.: Dynamique des sels nutritifs et de la matière organique dans le système fluvioestuarien de l'Adour/Golfe de Gascogne, Université de Pau et des Pays de l'adour, 2019.

Dodds, W. K. and Smith, V. H.: Nitrogen, phosphorus, and eutrophication in streams, Inland Waters, 6, 155–164, https://doi.org/10.5268/IW-6.2.909, 2016.

Dubois, S., Savoye, N., Grémare, A., Plus, M., Charlier, K., Beltoise, A., and Blanchet, H.: Origin and composition of sediment organic matter in a coastal semi-enclosed ecosystem: An elemental and isotopic study at the ecosystem space scale, Journal of Marine Systems, 94, 64–73, https://doi.org/10.1016/j.jmarsys.2011.10.009, 2012.

Dunn†, J. C.: Well-Separated Clusters and Optimal Fuzzy Partitions, Journal of Cybernetics, 4, 95–104, https://doi.org/10.1080/01969727408546059, 1974.

Dürr, H. H., Laruelle, G. G., van Kempen, C. M., Slomp, C. P., Meybeck, M., and Middelkoop, H.: Worldwide Typology of Nearshore Coastal Systems: Defining the Estuarine Filter of River Inputs to the Oceans, Estuaries and Coasts, 34, 441–458, https://doi.org/10.1007/s12237-011-9381-y, 2011.

Etcheber, H., Taillez, A., Abril, G., Garnier, J., Servais, P., Moatar, F., and Commarieu, M.-V.: Particulate organic carbon in the estuarine turbidity maxima of the Gironde, Loire and Seine estuaries: origin and lability, Hydrobiologia, 588, 245–259, https://doi.org/10.1007/s10750-007-0667-9, 2007.

Falkowski, P. G., Barber, R. T., and Smetacek, V.: Biogeochemical Controls and Feedbacks on Ocean Primary Production, Science, 281, 200–206, https://doi.org/10.1126/science.281.5374.200, 1998.

Ferchiche, F., Liénart, C., Charlier, K., Coynel, A., Gorse-Labadie, L., and Savoye, N.: Quantifying particulate organic matter: source composition and fluxes at the river-estuary interface, Front. Freshw. Sci., 2, https://doi.org/10.3389/ffwsc.2024.1437431, 2024.

Ferchiche, F., Liénart, C., Savoye, N., and Wassenaar, L. I.: Unlocking the potential of hydrogen isotopes (δ2H) in tracing riverine particulate organic matter sources and dynamics, Aquat Sci, 87, 5, https://doi.org/10.1007/s00027-024-01127-1, 2025.

Fernandez, I., Mahieu, N., and Cadisch, G.: Carbon isotopic fractionation during decomposition of plant materials of different quality, Global Biogeochemical Cycles, 17, https://doi.org/10.1029/2001GB001834, 2003.

Field, C. B., Behrenfeld, M. J., Randerson, J. T., and Falkowski, P.: Primary Production of the Biosphere: Integrating Terrestrial and Oceanic Components, Science, 281, 237–240, https://doi.org/10.1126/science.281.5374.237, 1998.

Finlay, J. C., Doucett, R. R., and McNEELY, C.: Tracing energy flow in stream food webs using stable isotopes of hydrogen, Freshwater Biology, 55, 941–951, https://doi.org/10.1111/j.1365-2427.2009.02327.x, 2010.

Fry, B.: 13C/12C fractionation by marine diatoms, Marine Ecology Progress Series, 134, 283–294, https://doi.org/10.3354/meps134283, 1996.

Galeron, M.-A., Radakovitch, O., Charrière, B., Vaultier, F., and Rontani, J.-F.: Autoxidation as a major player in the fate of terrestrial particulate organic matter in seawater, Journal of Geophysical Research: Biogeosciences, 122, 1203–1215, https://doi.org/10.1002/2016JG003708, 2017.

Gawade, L., Krishna, M. S., Sarma, V. V. S. S., Hemalatha, K. P. J., and Venkateshwara Rao, Y.: Spatio-temporal variability in the sources of particulate organic carbon and nitrogen in a tropical Godavari estuary, Estuarine, Coastal and Shelf Science, 215, 20–29, https://doi.org/10.1016/j.ecss.2018.10.004, 2018.

Golubkov, M. S., Nikulina, V. N., Tiunov, A. V., and Golubkov, S. M.: Stable C and N Isotope Composition of Suspended Particulate Organic Matter in the Neva Estuary: The Role of Abiotic Factors, Productivity, and Phytoplankton Taxonomic Composition, Journal of Marine Science and Engineering, 8, 959, https://doi.org/10.3390/jmse8120959, 2020.

Goñi, M. A., Voulgaris, G., and Kim, Y. H.: Composition and fluxes of particulate organic matter in a temperate estuary (Winyah Bay, South Carolina, USA) under contrasting physical forcings, Estuarine, Coastal and Shelf Science, 85, 273–291, https://doi.org/10.1016/j.ecss.2009.08.013, 2009.

Govan, E. and Parnell, A.: simmr: A Stable Isotope Mixing Model, 2024.

Grunicke, F., Wagner, A., von Elert, E., Weitere, M., and Berendonk, T.: Riparian detritus vs. stream detritus: food quality determines fitness of juveniles of the highly endangered freshwater pearl mussels (Margaritifera margaritifera), Hydrobiologia, 850, 729–746, https://doi.org/10.1007/s10750-022-05120-3, 2023.

Harmelin-Vivien, M., Dierking, J., Bănaru, D., Fontaine, M. F., and Arlhac, D.: Seasonal variation in stable C and N isotope ratios of the Rhone River inputs to the Mediterranean Sea (2004–2005), Biogeochemistry, 100, 139–150, https://doi.org/10.1007/s10533-010-9411-z, 2010.

Hellings, L., Dehairs, F., Tackx, M., Keppens, E., and Baeyens, W.: Origin and fate of organic carbon in the freshwater part of the Scheldt Estuary as traced by stable carbon isotope composition, Biogeochemistry, 47, 167–186, https://doi.org/10.1023/A:1006143827118, 1999.

Higueras, M., Kerhervé, P., Sanchez-Vidal, A., Calafat, A., Ludwig, W., Verdoit-Jarraya, M., Heussner, S., and Canals, M.: Biogeochemical characterization of the riverine particulate organic matter transferred to the NW Mediterranean Sea, Biogeosciences, 11, 157–172, https://doi.org/10.5194/bg-11-157-2014, 2014.

Hilton, R. G., Galy, A., Hovius, N., Horng, M.-J., and Chen, H.: The isotopic composition of particulate organic carbon in mountain rivers of Taiwan, Geochimica et Cosmochimica Acta, 74, 3164–3181, https://doi.org/10.1016/j.gca.2010.03.004, 2010.

Hou, P., Eglinton, T. I., Yu, M., Montluçon, D. B., Haghipour, N., Zhang, H., Jin, G., and Zhao, M.: Degradation and Aging of Terrestrial Organic Carbon within Estuaries:

Biogeochemical and Environmental Implications, Environmental Science and Technology, 55, 10852–10861, https://doi.org/10.1021/acs.est.1c02742, 2021.

Hounshell, A. G., Fegley, S. R., Hall, N. S., Osburn, C. L., and Paerl, H. W.: Riverine Discharge and Phytoplankton Biomass Control Dissolved and Particulate Organic Matter Dynamics over Spatial and Temporal Scales in the Neuse River Estuary, North Carolina, Estuaries and Coasts, 45, 96–113, https://doi.org/10/gj64px, 2022.

INRA: Base de Données Géographique des Sols de France à 1/1 000 000 version 3.2.8.0, 10/09/1998, https://doi.org/10.15454/BPN57S, 2025.

Kang, S., Kim, J.-H., Joe, Y. J., Jang, K., Nam, S.-I., and Shin, K.-H.: Long-term environmental changes in the Geum Estuary (South Korea): Implications of river impoundments, Marine Pollution Bulletin, 168, 112383, https://doi.org/10/gnpb2t, 2021.

Ke, Z., Tan, Y., Huang, L., Liu, J., Xiang, C., Zhao, C., and Zhang, J.: Significantly depleted 15N in suspended particulate organic matter indicating a strong influence of sewage loading in Daya Bay, China, Science of The Total Environment, 650, 759–768, https://doi.org/10.1016/j.scitotenv.2018.09.076, 2019.

Kelso, J. E. and Baker, M. A.: Organic Matter Is a Mixture of Terrestrial, Autochthonous, and Wastewater Effluent in an Urban River, Frontiers in Environmental Science, 7, https://doi.org/10.3389/fenvs.2019.00202, 2020.

Kelso, J. E. and Baker, M. A.: Organic matter sources and composition in four watersheds with mixed land cover, Hydrobiologia, 849, 2663–2682, https://doi.org/10.1007/s10750-022-04884-y, 2022.

Kendall, C., Silva, S. R., and Kelly, V. J.: Carbon and nitrogen isotopic compositions of particulate organic matter in four large river systems across the United States, Hydrological Processes, 15, 1301–1346, https://doi.org/10.1002/hyp.216, 2001.

Khan, M. N. and Mohammad, F.: Eutrophication: Challenges and Solutions, in: Eutrophication: Causes, Consequences and Control: Volume 2, edited by: Ansari, A. A. and Gill, S. S., Springer Netherlands, Dordrecht, 1–15, https://doi.org/10.1007/978-94-007-7814-6_1, 2014.

Lambert, T., Bouillon, S., Darchambeau, F., Morana, C., Roland, F. A. E., Descy, J.-P., and Borges, A. V.: Effects of human land use on the terrestrial and aquatic sources of fluvial organic matter in a temperate river basin (The Meuse River, Belgium), Biogeochemistry, 136, 191–211, https://doi.org/10.1007/s10533-017-0387-9, 2017.

Le Bas, C.: Carte de la Réserve Utile en eau issue de la Base de Données Géographique des Sols de France, https://doi.org/10.15454/JPB9RB, 2025.

Lebreton, B., Beseres Pollack, J., Blomberg, B., Palmer, T. A., Adams, L., Guillou, G., and Montagna, P. A.: Origin, composition and quality of suspended particulate organic matter in relation to freshwater inflow in a South Texas estuary, Estuarine, Coastal and Shelf Science, 170, 70–82, https://doi.org/10.1016/j.ecss.2015.12.024, 2016.

Legendre, P., Oksanen, J., and ter Braak, C. J. F.: Testing the significance of canonical axes in redundancy analysis, Methods in Ecology and Evolution, 2, 269–277, https://doi.org/10.1111/j.2041-210X.2010.00078.x, 2011.

Lheureux, A., David, V., Del Amo, Y., Soudant, D., Auby, I., Ganthy, F., Blanchet, H., Cordier, M.-A., Costes, L., Ferreira, S., Mornet, L., Nowaczyk, A., Parra, M., D'Amico, F., Gouriou, L., Meteigner, C., Oger-Jeanneret, H., Rigouin, L., Rumebe, M., Tournaire, M.-P., Trut, F., Trut, G., and Savoye, N.: Bi-decadal changes in nutrient concentrations and ratios in marine coastal ecosystems: The case of the Arcachon bay, France, Progress in Oceanography, 201, 102740, https://doi.org/10.1016/j.pocean.2022.102740, 2022.

Liénart, C., Susperregui, N., Rouaud, V., Cavalheiro, J., David, V., Del Amo, Y., Duran, R., Lauga, B., Monperrus, M., Pigot, T., Bichon, S., Charlier, K., and Savoye, N.: Dynamics of particulate organic matter in a coastal system characterized by the occurrence of marine mucilage – A stable isotope study, Journal of Sea Research, 116, 12–22, https://doi.org/10.1016/j.seares.2016.08.001, 2016.

Liénart, C., Savoye, N., Bozec, Y., Breton, E., Conan, P., David, V., Feunteun, E., Grangeré, K., Kerhervé, P., Lebreton, B., Lefebvre, S., L'Helguen, S., Mousseau, L., Raimbault, P., Richard, P., Riera, P., Sauriau, P.-G., Schaal, G., Aubert, F., Aubin, S., Bichon, S., Boinet, C., Bourasseau, L., Bréret, M., Caparros, J., Cariou, T., Charlier, K., Claquin, P., Cornille, V., Corre, A.-M., Costes, L., Crispi, O., Crouvoisier, M., Czamanski, M., Del Amo, Y., Derriennic, H., Dindinaud, F., Durozier, M., Hanquiez, V., Nowaczyk, A., Devesa, J., Ferreira, S., Fornier, M., Garcia, F., Garcia, N., Geslin, S., Grossteffan, E., Gueux, A., Guillaudeau, J., Guillou, G., Joly, O., Lachaussée, N., Lafont, M., Lamoureux, J., Lecuyer, E., Lehodey, J.-P., Lemeille, D., Leroux, C., Macé, E., Maria, E., Pineau, P., Petit, F., Pujo-Pay, M., Rimelin-Maury, P., and Sultan, E.: Dynamics of particulate organic matter composition in coastal systems: A spatio-temporal study at multi-systems scale, Progress in Oceanography, 156, 221–239, https://doi.org/10/gb27ss, 2017.

Liénart, C., Savoye, N., David, V., Ramond, P., Rodriguez Tress, P., Hanquiez, V., Marieu, V., Aubert, F., Aubin, S., Bichon, S., Boinet, C., Bourasseau, L., Bozec, Y., Bréret, M., Breton, E., Caparros, J., Cariou, T., Claquin, P., Conan, P., Corre, A.-M., Costes, L., Crouvoisier, M., Del Amo, Y., Derriennic, H., Dindinaud, F., Duran, R., Durozier, M., Devesa, J., Ferreira, S., Feunteun, E., Garcia, N., Geslin, S., Grossteffan, E., Gueux, A., Guillaudeau, J., Guillou, G., Jolly, O., Lachaussée, N., Lafont, M., Lagadec, V., Lamoureux, J., Lauga, B., Lebreton, B., Lecuyer, E., Lehodey, J.-P., Leroux, C., L'Helguen, S., Macé, E., Maria, E., Mousseau, L., Nowaczyk, A., Pineau, P., Petit, F., Pujo-Pay, M., Raimbault, P., Rimmelin-Maury, P., Rouaud, V., Sauriau, P.-G., Sultan, E., and Susperregui, N.: Dynamics of particulate organic matter composition in coastal systems: Forcing of spatio-temporal variability at multi-systems scale, Progress in Oceanography, 162, 271–289, https://doi.org/10.1016/j.pocean.2018.02.026, 2018.

Liénart, C., Savoye, N., Conan, P., David, V., Barbier, P., Bichon, S., Charlier, K., Costes, L., Derriennic, H., Ferreira, S., Gueux, A., Hubas, C., Maria, E., and Meziane, T.: Relationship between bacterial compartment and particulate organic matter (POM) in coastal systems: An assessment using fatty acids and stable isotopes, Estuarine, Coastal and Shelf Science, 239, 106720, https://doi.org/10.1016/j.ecss.2020.106720, 2020.

1077 Lowe, A. T., Galloway, A. W. E., Yeung, J. S., Dethier, M. N., and Duggins, D. O.: Broad
1078 sampling and diverse biomarkers allow characterization of nearshore particulate organic
1079 matter, Oikos, 123, 1341–1354, https://doi.org/10.1111/oik.01392, 2014.

1080 Lu, L., Cheng, H., Pu, X., Wang, J., Cheng, Q., and Liu, X.: Identifying organic matter
1081 sources using isotopic ratios in a watershed impacted by intensive agricultural activities in
1082 Northeast China, Agriculture, Ecosystems & Environment, 222, 48–59,
1083 https://doi.org/10.1016/j.agee.2015.12.033, 2016.

1084 McCorkle, E. P., Berhe, A. A., Hunsaker, C. T., Johnson, D. W., McFarlane, K. J., Fogel, M.
1085 L., and Hart, S. C.: Tracing the source of soil organic matter eroded from temperate forest
1086 catchments using carbon and nitrogen isotopes, Chemical Geology, 445, 172–184,
1087 https://doi.org/10.1016/j.chemgeo.2016.04.025, 2016.

1088 Michener, R. H. and Kaufman, L.: Stable Isotope Ratios as Tracers in Marine Food Webs: An
1089 Update, 1st ed., edited by: Michener, R. and Lajtha, K., Wiley,
1090 https://doi.org/10.1002/9780470691854.ch9, 2007.

1091 Middelburg, J. J. and Herman, P. M. J.: Organic matter processing in tidal estuaries, Marine
1092 Chemistry, 106, 127–147, https://doi.org/10.1016/j.marchem.2006.02.007, 2007.

1093 Miller, R. J., Page, H. M., and Brzezinski, M. A.: δ13C and δ15N of particulate organic
1094 matter in the Santa Barbara Channel: drivers and implications for trophic inference, Marine
1095 Ecology Progress Series, 474, 53–66, https://doi.org/10.3354/meps10098, 2013.

1096 Minaudo, C., Meybeck, M., Moatar, F., Gassama, N., and Curie, F.: Eutrophication mitigation
1097 in rivers: 30 years of trends in spatial and seasonal patterns of biogeochemistry of the Loire
1098 River (1980–2012), Biogeosciences, 12, 2549–2563, https://doi.org/10.5194/bg-12-2549-
1099 2015, 2015.

1100 Minaudo, C., Moatar, F., Coynel, A., Etcheber, H., Gassama, N., and Curie, F.: Using recent
1101 high-frequency surveys to reconstitute 35 years of organic carbon variations in a eutrophic
1102 lowland river, Environ Monit Assess, 188, 41, https://doi.org/10.1007/s10661-015-5054-9,
1103 2016.

1104 Ogrinc, N., Markovics, R., Kanduč, T., Walter, L. M., and Hamilton, S. K.: Sources and
1105 transport of carbon and nitrogen in the River Sava watershed, a major tributary of the River
1106 Danube, Applied Geochemistry, 23, 3685–3698,
1107 https://doi.org/10.1016/j.apgeochem.2008.09.003, 2008.

1108 O'Leary, M. H.: Carbon isotope fractionation in plants, Phytochemistry, 20, 553–567,
1109 https://doi.org/10.1016/0031-9422(81)85134-5, 1981.

1110 Onstad, G. D., Canfield, D. E., Quay, P. D., and Hedges, J. I.: Sources of particulate organic
1111 matter in rivers from the continental usa: lignin phenol and stable carbon isotope
1112 compositions, Geochimica et Cosmochimica Acta, 64, 3539–3546,
1113 https://doi.org/10.1016/S0016-7037(00)00451-8, 2000.

1114 Parnell, A. C., Phillips, D. L., Bearhop, S., Semmens, B. X., Ward, E. J., Moore, J. W.,
1115 Jackson, A. L., Grey, J., Kelly, D. J., and Inger, R.: Bayesian stable isotope mixing models,
1116 Environmetrics, 24, 387–399, https://doi.org/10.1002/env.2221, 2013.

1117 Perdue, E. M. and Koprivnjak, J.-F.: Using the C/N ratio to estimate terrigenous inputs of
1118 organic matter to aquatic environments, Estuarine, Coastal and Shelf Science, 73, 65–72,
1119 https://doi.org/10.1016/j.ecss.2006.12.021, 2007.

1120 Phillips, D. L., Inger, R., Bearhop, S., Jackson, A. L., Moore, J. W., Parnell, A. C., Semmens,
1121 B. X., and Ward, E. J.: Best practices for use of stable isotope mixing models in food-web
1122 studies, Can. J. Zool., 92, 823–835, https://doi.org/10.1139/cjz-2014-0127, 2014.

1123 Polsenaere, P., Savoye, N., Etcheber, H., Canton, M., Poirier, D., Bouillon, S., and Abril, G.:
1124 Export and degassing of terrestrial carbon through watercourses draining a temperate
1125 podzolized catchment, Aquat Sci, 75, 299–319, https://doi.org/10.1007/s00027-012-0275-2,
1126 2013.

1127 Pradhan, U. K., Wu, Y., Wang, X., Zhang, J., and Zhang, G.: Signals of typhoon induced
1128 hydrologic alteration in particulate organic matter from largest tropical river system of Hainan
1129 Island, South China Sea, Journal of Hydrology, 534, 553–566,
1130 https://doi.org/10.1016/j.jhydrol.2016.01.046, 2016.

1131 Regnier, P., Friedlingstein, P., Ciais, P., Mackenzie, F. T., Gruber, N., Janssens, I. A.,
1132 Laruelle, G. G., Lauerwald, R., Luyssaert, S., Andersson, A. J., Arndt, S., Arnosti, C., Borges,
1133 A. V., Dale, A. W., Gallego-Sala, A., Goddéris, Y., Goossens, N., Hartmann, J., Heinze, C.,
1134 Ilyina, T., Joos, F., LaRowe, D. E., Leifeld, J., Meysman, F. J. R., Munhoven, G., Raymond,
1135 P. A., Spahni, R., Suntharalingam, P., and Thullner, M.: Anthropogenic perturbation of the
1136 carbon fluxes from land to ocean, Nature Geosci, 6, 597–607,
1137 https://doi.org/10.1038/ngeo1830, 2013.

1138 Rousseeuw, P. J.: Silhouettes: A graphical aid to the interpretation and validation of cluster
1139 analysis, Journal of Computational and Applied Mathematics, 20, 53–65,
1140 https://doi.org/10.1016/0377-0427(87)90125-7, 1987.

1141 Sarma, V. V. S. S., Krishna, M. S., Prasad, V. R., Kumar, B. S. K., Naidu, S. A., Rao, G. D.,
1142 Viswanadham, R., Sridevi, T., Kumar, P. P., and Reddy, N. P. C.: Distribution and sources of
1143 particulate organic matter in the Indian monsoonal estuaries during monsoon, Journal of
1144 Geophysical Research: Biogeosciences, 119, 2095–2111,
1145 https://doi.org/10.1002/2014JG002721, 2014.

1146 Sato, T., Miyajima, T., Ogawa, H., Umezawa, Y., and Koike, I.: Temporal variability of
1147 stable carbon and nitrogen isotopic composition of size-fractionated particulate organic matter
1148 in the hypertrophic Sumida River Estuary of Tokyo Bay, Japan, Estuarine, Coastal and Shelf
1149 Science, 68, 245–258, https://doi.org/10.1016/j.ecss.2006.02.007, 2006.

1150 Savoye, N., Aminot, A., Tréguer, P., Fontugne, M., Naulet, N., and Kérouel, R.: Dynamics of
1151 particulate organic matter d15N and d13C during spring phytoplankton blooms in a
1152 macrotidal ecosystem (Bay of Seine, France), Marine Ecology Progress Series, 255, 27–41,
1153 https://doi.org/10.3354/meps255027, 2003.

1154 Savoye, N., David, V., Morisseau, F., Etcheber, H., Abril, G., Billy, I., Charlier, K., Oggian,
1155 G., Derriennic, H., and Sautour, B.: Origin and composition of particulate organic matter in a
1156 macrotidal turbid estuary: The Gironde Estuary, France, Estuarine, Coastal and Shelf Science,
1157 108, 16–28, https://doi.org/10.1016/j.ecss.2011.12.005, 2012.

Sigman, D. M., DiFiore, P. J., Hain, M. P., Deutsch, C., Wang, Y., Karl, D. M., Knapp, A. N., Lehmann, M. F., and Pantoja, S.: The dual isotopes of deep nitrate as a constraint on the cycle and budget of oceanic fixed nitrogen, Deep Sea Research Part I: Oceanographic Research Papers, 56, 1419–1439, https://doi.org/10.1016/j.dsr.2009.04.007, 2009.

Souissi, S., Yahia-Kéfi, O. D., and Yahia, M. N. D.: Spatial characterization of nutrient dynamics in the Bay of Tunis (south-western Mediterranean) using multivariate analyses: consequences for phyto- and zooplankton distribution, Journal of Plankton Research, 22, 2039–2059, https://doi.org/10.1093/plankt/22.11.2039, 2000.

Sun, X., Fan, D., Cheng, P., Hu, L., Sun, X., Guo, Z., and Yang, Z.: Source, transport and fate of terrestrial organic carbon from Yangtze River during a large flood event: Insights from multiple-isotopes (δ13C, δ15N, Δ14C) and geochemical tracers, Geochimica et Cosmochimica Acta, 308, 217–236, https://doi.org/10/gn8qs5, 2021.

Turner, R. E., Milan, C. S., Swenson, E. M., and Lee, J. M.: Peak chlorophyll a concentrations in the lower Mississippi River from 1997 to 2018, Limnology and Oceanography, n/a, https://doi.org/10/gpjm83, 2022.

Veyssy, E., Etcheber, H., Lin, R. G., Buat-Menard, P., and Maneux, E.: Seasonal variation and origin of Particulate Organic Carbon in the lower Garonne River at La Reole (southwestern France), Hydrobiologia, 391, 113–126, https://doi.org/10.1023/A:1003520907962, 1998.

Wang, X., Chen, Y., Yuan, Q., Xing, X., Hu, B., Gan, J., Zheng, Y., and Liu, Y.: Effect of river damming on nutrient transport and transformation and its countermeasures, Frontiers in Marine Science, 9, 2022.

Wang, Y., Song, J., Duan, L., Yuan, H., Li, X., Li, N., Zhang, Q., Liu, J., and Ren, C.: Combining sterols with stable carbon isotope as indicators for assessing the organic matter sources and primary productivity evolution in the coastal areas of the East China Sea, Continental Shelf Research, 223, 104446, https://doi.org/10.1016/j.csr.2021.104446, 2021.

Yaalon, D. H.: Soils in the Mediterranean region: what makes them different?, CATENA, 28, 157–169, https://doi.org/10.1016/S0341-8162(96)00035-5, 1997.

Yan, X., Yang, J.-Y. T., Xu, M. N., Wang, H., Dai, M., and Kao, S.-J.: Nitrogen isotope constraint on the zonation of multiple transformations between dissolved and particulate organic nitrogen in the Changjiang plume, Science of The Total Environment, 818, 151678, https://doi.org/10.1016/j.scitotenv.2021.151678, 2022.

Yu, F., Zong, Y., Lloyd, J. M., Huang, G., Leng, M. J., Kendrick, C., Lamb, A. L., and Yim, W. W.-S.: Bulk organic δ13C and C/N as indicators for sediment sources in the Pearl River delta and estuary, southern China, Estuarine, Coastal and Shelf Science, 87, 618–630, https://doi.org/10.1016/j.ecss.2010.02.018, 2010.

Zhang, Y., Meng, X., Bai, Y., Wang, X., Xia, P., Yang, G., Zhu, Z., and Zhang, H.: Sources and features of particulate organic matter in tropical small mountainous rivers (SW China) under the effects of anthropogenic activities, Ecological Indicators, 125, 107471, https://doi.org/10.1016/j.ecolind.2021.107471, 2021.

1199